Microscopic solvation effects on excitedstate energetics and dynamics of aromatic molecules in large van der Waals complexes

A. Amirav, U. Even, and Joshua Jortner

Citation: The Journal of Chemical Physics **75**, 2489 (1981); doi: 10.1063/1.442426
View online: http://dx.doi.org/10.1063/1.442426
View Table of Contents: http://scitation.aip.org/content/aip/journal/jcp/75/6?ver=pdfcov
Published by the AIP Publishing

Microscopic solvation effects on excited-state energetics and dynamics of aromatic molecules in large van der Waals complexes

A. Amirav, U. Even, and Joshua Jortner

Department of Chemistry, Tel-Aviv University, Tel Aviv, Israel
(Received 29 December 1980; accepted 4 March 1981)

In this paper we report the results of an experimental study of the formation kinetics, excited-state energetics, interstate electronic relaxation, and intrastate nuclear dynamics in electronically–vibrationally excited states of van der Waals molecules, consisting of a tetracene(T) molecule and rare-gas (R) atoms. The TR_n molecules were synthesized in seeded supersonic jets. Excited-state energetics and dynamics of TR_n molecules were explored by laser spectroscopy in supersonic expansions, interrogating the fluorescence action spectra, the energy-resolved emission, the relative emission quantum yields, and the time-resolved emission. Spectroscopic diagnostic methods for the identification and characterization of the chemical composition of TR_n complexes involved the dependence of the spectral features on the identity of the rare gas, an intensity conservation rule for the intensities of TAr_n and of T, the pressure dependence of the intensity of the bare T molecule, the pressure dependence of the intensity of the spectral features of the TR_n molecules, and their order of appearance. We were able to identify the following 13 molecules: TAr_n ($n = 1,2,\cdots 7$), TKr_n ($n = 1,2,3,4$), and TXe_n ($n = 1,2$), and to assign the spectral features which correspond to the vibrationless $S_0 \rightarrow S_1$ excitations of these molecules. For TAr_1, TAr_2, TAr_3, TKr_1, and TKr_2, a single spectral feature corresponding to each molecule was observed, providing evidence against the existence of distinct chemical isomers of these molecules. For TKr_3 and TKr_4 a multiple spectrum consisting of several bands for each chemical composition was observed, which was tentatively assigned to chemical isomers of these molecules. The TXe_1 and TXe_2 spectra reveal, in addition to a main band, weak satellites which were tentatively attributed to vibrational structure. The red spectral shifts of the vibrationless and the 314 cm^{-1} $S_0 \rightarrow S_1$ electronic excitations of all TR_n molecules from the corresponding excitation of the bare T molecule are dominated by dispersive interactions, the red shifts for the TR_1 (R = Ne, Ar, Kr, and Xe) molecules being proportional to the polarizability of the R atom. The spectral shifts of TR_n molecules are not additive per added atom, the violation of the additivity law being attributed to the occupation of geometrically inequivalent sites by the R atoms. To demonstrate the universality of van der Waals molecule formation by large aromatics, we have studied the energetics of $T(N_2)_n$ ($n = 1$–3) molecules and obtained preliminary spectroscopic data on $T(C_6H_6)$ and $T(H_2O)$. We have studied, subsequently, microscopic solvent effects on electronic relaxation from the vibrationless S_1 state and from the 314 cm^{-1} vibrational excitation of this state of tetracene embedded in well characterized TR_n complexes. The decay lifetimes τ of the vibrationless S_1 electronic state of TNe_1 and TAr_n ($n = 1,2,\cdots 7$) molecules are in the range $\tau = 17 \pm 2$ to 34 ± 3 nsec, being close to or somewhat higher than the lifetime $\tau_0 = 19 \pm 2$ nsec of the electronic origin of the bare T molecule. The lifetimes of the vibrationless level of TKr_1, TKr_2, TKr_3, and TKr_4 molecules ($\tau = 6 \pm 1$ to 8 ± 1 nsec) and of TXe_1 and TXe_2 complexes ($\tau \sim 1.5$ nsec) reveal a dramatic shortening relative to τ_0, which is attributed to the heavy atom enhancement of $S_1 \rightarrow T_1$ crossing. The lifetimes of TKr_n ($n = 1$–4) and of TXe_n are practically independent of the coordination number, whereupon the heavy atom enhancement of intersystem crossing in these systems essentially originates from T–Kr and T–Xe single-pair interactions. We also explored some effects of intrastate nuclear dynamics in the S_1 state of TAr_n and of TKr_n molecules. We have demonstrated that the 314 cm^{-1} vibrational excitations of TAr_1 and of TKr_1 do not result in vibrational predissociation on the (nsec) time scale of the excited-state lifetime, the reactive channel being presumably closed. The heavy atom effect on the decay lifetimes of TKr_n was utilized to search for the onset of vibrational predissociation, which is exhibited at excess vibrational energies of 1250 cm^{-1} above the electronic origin.

I. INTRODUCTION

Considerable effort in the broad area of physical chemistry was directed towards the elucidation of solvent effects on the energetics and intramolecular dynamics of vibrationally–electronically excited guest molecules embedded in solutions, glasses, and solids. In this context extensive studies of excited-state energetics of molecules in a condensed medium were conducted exploring spectral shifts of electronic energy levels[1–3] and solvent perturbations of intramolecular vibrational frequencies.[4] Studies of medium effects on excited-state dynamics considered a broad spectrum of photophysical phenomena, such as solvent effects on radiative lifetimes,[5] solvent-induced electronic relaxation in molecules corresponding to the intermediate level structure,[6,7] solvent perturbations of electronic relaxation in molecules, which correspond to the statistical limit,[6,8] and medium-induced molecular vibrational relaxation.[9] The information emerging from such studies is inherently limited because of several reasons. First, the cumulative effects exerted by the host medium on the guest molecule consist of a superposition of individual pair (or higher-order) contributions from the distinct solvent species. Second, the host–guest interactions are determined by the local structure of the solvent around the solute. Third, the guest–host interactions may be complicated by dynamic motion of the solvent, i.e., phonon

 0021-9606/81/182489-24$01.00

coupling effects. Consequently, the microscopic information regarding the effects of intermolecular interactions on energetics and intramolecular dynamics cannot readily be disentangled from traditional experimental data on solvent perturbations in a dense medium. Solvent effects on excited-state energetics and dynamics can be studied by embedding a "guest" molecule in a van der Waals (vdW) complex, rather than in a dense medium. vdW molecules[10–18] are weakly bound molecular complexes held together by attractive interactions (e.g., dispersive, electrostatic, charge transfer, hydrogen bonding) between closed-shell atoms or molecules. The primary characteristics of vdW bonds are their low (10–1000 cm^{-1}) dissociative energies, the long bond length, and the retention of many of the individual properties of the molecular constituents within the vdW complex.[10,13] Consequently, a vdW complex consisting of a diatomic or polyatomic molecule and simple ligand(s), such as rare-gas atoms, can be viewed as a guest molecule embedded in a well-characterized local solvent configuration whose excited-state features can be studied.

Supersonic expansion beams offer an excellent medium for the production of a variety of fascinating weakly bound vdW molecules[10–16] and molecular clusters.[19,20] During the last few years there have been extensive studies of the ground state structure and energetics,[10,21,22] the excited-state energetics,[13,18,19] as well as the dynamics of vibrational predissociation[13–15,17,18,23,24] of vdW molecules. Studies of the energetics and intramolecular dynamics of vdW molecules are expected to yield basic information on solvent perturbations as explored from the microscopic point of view. With this goal in mind, we have undertaken an experimental study of the formation kinetics, the energetics, and intramolecular dynamics in vibrationally–electronically excited states of vdW molecules consisting of large aromatic molecules, such as anthracene, tetracene, or pentacene, and rare-gas atoms. These large vdW molecules were synthesized in seeded supersonic expansions. By an appropriate choice of the stagnation pressure and of the nozzle diameter, we were able to accomplish selective, gradual, and controlled solvation of an aromatic molecule with rare-gas atoms. The most extensive data were obtained for the tetracene(T)–rare-gas(R) vdW molecules, which constitute the main theme of the present paper. The experimental interrogation techniques are based on energy-resolved and time-resolved spectroscopy in supersonic expansions,[25,26] monitoring photoselected states of well-defined TR_n molecules in their first electronically excited singlet configuration. The major accomplishments of the present study can be summarized as follows:

Synthesis: Studies of the formation kinetics of TR_n molecules provided diagnostic spectroscopic criteria for the identification of the individual vdW complexes. The quantitative aspects of the formation kinetics of large vdW TR_n molecules are of interest for the understanding of nucleation processes, as approached from the microscopic point of view.

Spectral shifts: The investigation of the excitation energies of the individual $T–R_n$ complexes provides interesting information on the spectral shifts exerted by rare gases on the $S_0 \rightarrow S_1$ excitation of T. In contrast to the extensive work on solvent shifts,[1–3] the present study provides direct information on molecule–solvent interactions in well-defined systems, providing a novel approach for exploring spectral solvent shifts from the microscopic point of view.

Solvent effects on electronic relaxation: We have studied the consequences of microscopic solvent perturbations excited by an "inert" solvent on electronic relaxation in the S_1 state of tetracene by investigating the effects of vdW complexing on the time-resolved emission from the vibrationless S_1 state of individual TR_n complexes. We have recorded modest solvent effects, i.e., changes in the decay lifetimes ~50%, on the lifetime of the S_1 electronic origin of T in TNe_n and TAr_n complexes, as compared to the lifetime of the S_1 electronic origin of the bare T molecule.

The heavy atom effect: We have demonstrated[16] the occurrence of the external heavy atom effect[27–37] on the $S_1 - T_1$ electronic relaxation of T in "isolated" TKr_n and TXe_n complexes in supersonic expansions by observing a dramatic shortening of the emission lifetimes and a reduction in the emission quantum yields from the S_1 electronic origin of T in these complexes. These studies provide a novel approach for exploring microscopic solvent effects in electronic relaxation.

Intramolecular vibrational energy redistribution: Nonreactive intramolecular vibrational energy flow in TAr_n complexes at low levels of vibrational excitation was investigated by probing the energy-resolved emission. Photoselection of low-lying vibrationally excited states below the T–Ar dissociation energy results in vibrational energy redistribution in the vdW complex.

Decomposition of vibrationally excited complexes: Reactive vibrational predissociation (VP) of TKr_n complexes was studied by probing the time-resolved emission. Utilization of the external heavy atom effect on electronic relaxation enabled us to distinguish between the decay of the complex and the decay of the bare molecule, which results from VP of the TKr complex. These studies provide some information on the bonding energies of R atoms to large aromatic molecules.

These studies of excited-state energetics and dynamics of large TR_n vdW complexes in supersonic beams are of considerable interest for establishing relations and correlations between the energetic and dynamic features of free molecules and of those molecules in condensed phases.

II. EXPERIMENTAL DETAILS

The experimental techniques developed in our laboratory for laser spectroscopy in supersonic expansions were already described in detail.[25,26] Briefly, our supersonic beam apparatus uses a 6 in. diffusion pump (Varian VHS 6) backed by a (Alcaltel) rotating pump with a pumping speed of 500 liter min^{-1}. This pumping system was utilized for supersonic free expansions through a $D = 150$ μ nozzle of Ar, Kr, and Xe at the stagnation

pressures of $p = 50-1500$ Torr. For some high flow experiments, where seeded Ne and nitrogen were expanded at $p = 3000-8000$ Torr through the $D = 150$ μ nozzle, only the Alcaltel rotatory pump was employed.[25] A gaseous mixture of the diluent gas at $p = 50-1500$ Torr for Ar, Kr, and Xe and $p = 3000-8000$ Torr for Ne and N_2 seeded with tetracene, which was heated in the sample chamber to 220 °C (vapor pressure 10^{-1} Torr[38]), was expanded through the nozzle. The diluent gas was sent through a stainless steel chamber containing the heated solid sample of tetracene. The mixing of the diluent with the seeding molecule is effective to ensure a constant partial pressure of tetracene in the gaseous mixture prior to the supersonic expansion. The assumption of a constant partial pressure of the tetracene molecule in the gaseous mixture implies that the solubility[39] of the aromatic molecule in the diluent is small. On the basis of the quantitative data for the solubility of naphthalene in compressed gases,[39] we estimate that at $p = 1000$ Torr the solubility of this aromatic molecule will increase its concentration by 2%, which is negligible. Thus, in the pressure range $p = 100-1000$ Torr, where we shall provide a quantitative analysis of the experimental data, the partial pressure of the tetracene molecule can be safely assumed to be constant.

Our interrogation methods are based on monitoring the fluorescence action spectrum, the time-resolved fluorescence, and the energy-resolved fluorescence following laser photoselective excitation. The seeded supersonic expansion was crossed by a nitrogen pumped pulsed dye laser (Molectron DL2) with a spectral width of 0.3 cm^{-1} and a temporal Gaussian pulse shape with a pulse width (HWHM) of 4 nsec. In most of our experiments performed at the stagnation pressure of $p = 50-1500$ Torr the laser crossed the supersonic beam at 7 mm down the nozzle. In some experiments performed at $p = 3000-8000$ Torr the laser crossed the beam at 3.5 mm down the nozzle. The fluorescence was collected through a lens and detected by a photomultiplier. The fluorescence action spectrum, corresponding to the intensity of the total fluorescence vs the continuously scanned laser wavelength, was recorded by a boxcar integrator after normalization to the laser intensity. Lifetimes were measured by a biomation transient recorder (model 8100) with a time resolution of 10 nsec/channel and were averaged by a home-built signal averager. The decay of the fluorescence signal was measured over 2–3 orders of magnitude. Lifetimes longer than 5 nsec could be determined with an accuracy of ±10% directly from the output of the signal averager. As demonstrated by numerical simulations for lifetimes longer than 5 nsec, no deconvolution procedures of the signal were required.[26] The energy-resolved fluorescence resulting from laser excitation of the seeded jet at a fixed wavelength was collected and imaged by a lens onto the entrance slit of a monochromator and detected by a photomultiplier. The spectral resolution of these energy-resolved fluorescence spectra was 7 Å (30 cm^{-1}), while the accuracy of the positions of the peaks of the individual spectral features was estimated to be ±10 cm^{-1}.

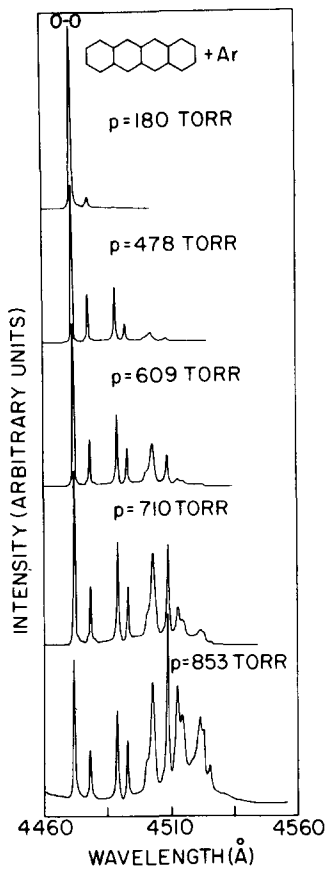

FIG. 1. Fluorescence excitation spectra of the $S_0 \rightarrow S_1$ electronic origin of tetracene and of TAr_n complexes in a supersonic expansion. Tetracene (at a fixed vapor pressure of 0.1 Torr) was seeded into Ar and expanded through a 150 μ nozzle. The backing pressures are indicated on the figure. The bandwidth of the exciting laser was 0.3 cm^{-1} and the laser crossed the supersonic jet 7 mm down the nozzle. All fluorescence excitation spectra are normalized to the laser intensity. The vibrationless 0–0 of the bare tetracene molecule at 4472 Å is marked 0–0. All these fluorescence excitation spectra were measured on an absolute intensity scale; the relative intensities I of the bare molecule 0–0 band are $I = 1.00$ at $p = 180$ Torr, $I = 0.50$ at $p = 478$ Torr, $I = 0.33$ at $p = 609$ Torr, $I = 0.20$ at $p = 710$ Torr, and $I = 0.10$ at $p = 853$ Torr.

III. SPECTROSCOPY OF TR_n van der WAALS COMPLEXES

Figures 1–3 portray the fluorescence excitation spectra in the range, 4460–4580 Å of tetracene seeded in supersonic expansions of Ar, Kr, and Xe, respectively. The spectra at $p = 180$ Torr of Ar, $p = 135$ Torr of Kr, and $p = 100$ Torr of Xe reveal a strong main feature peaking at 4472 Å, which is independent of the nature of the diluent gas. On the basis of our spectroscopic studies[26] of the ultracold tetracene molecule the 4472 Å feature is assigned to the electronic origin of the lowest spin-allowed $S_0(^1A_{1g}) \rightarrow S_1(^1B_{2u})$ transition of the isolated bare molecule. At the lowest pressure of the rare-gas diluents shown in Figs. 1–3, the internal cooling of the large molecule is efficient to eliminate all vibrational sequence congestion. Each of the spectra taken at these lowest pressures of the rare-gas diluents ($p = 180$ Torr

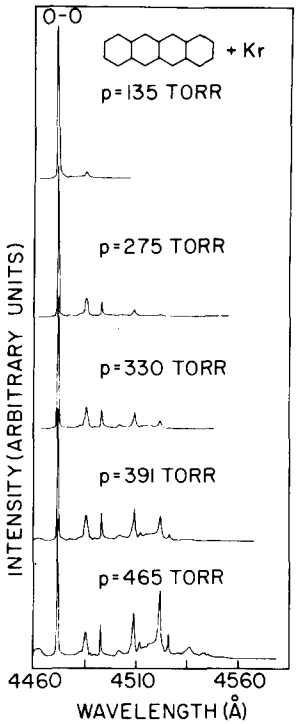

FIG. 2. Fluorescence excitation spectra of the $S_0 \rightarrow S_1$ electronic origin of tetracene and of TKr_n complexes. Tetracene (at a fixed vapor pressure ~ 0.1 Torr) was seeded in Kr and expanded through the 150 μ nozzle. All experimental conditions are as in Fig. 1. The vibrationless 0–0 excitation of bare tetracene at 4472 Å is marked 0–0. All these fluorescence excitation spectra were measured on an absolute intensity scale; the relative intensities I of the bare molecule 0–0 band are $I = 1.00$ at $p = 135$ Torr, $I = 0.50$ at $p = 275$ Torr, $I = 0.33$ at $p = 330$ Torr, $I = 0.20$ at $p = 391$ Torr, and $I = 0.10$ at $p = 465$ Torr.

Ar, $p = 135$ Torr Kr, and $p = 100$ Torr Xe) exhibits an additional single weak spectral feature which appears on the low energy side of the electronic origin of the bare molecule (Figs. 1–3). The red spectral shifts $\delta\nu$ for this satellite are $\delta\nu = 35$ cm^{-1} in Ar, $\delta\nu = 70$ cm^{-1} in Kr, and $\delta\nu = 101$ cm^{-1} in Xe. The weak satellite bands, which depend on the nature of the diluent gas, are tentatively attributed to the tetracene–rare-gas (TR) (R = Ar, Kr, and Xe) vdW molecule and this assignment will be borne out by the kinetic analysis of Sec. IV. Increasing the stagnation pressure of the heavy rare gas results in the appearance of a multitude of new spectral features on the low energy side of the 0–0 transition of the bare molecule (Figs. 1–3). Three general characteristics of these new spectral features should be noted. First, the energies of these spectral features depend on the identity of the diluent rare gas. Second, the intensities of the features exhibit a strong dependence on the stagnation pressure. Third, with increasing the stagnation pressure the spectral features at lower energies become more prominent. The new additional spectral features are attributed to TR_n (R ≡ Ar, Kr, and Xe) vdW molecules with various coordination numbers n. All the spectral features appearing on the low energy side of the electronic origin of the bare tetracene molecule are assigned to vibrationless 0–0 transitions of TR_n molecules. The interpretation is consistent with the dependence of the energies of the spectral features as the identity of the diluent and will be borne out by the quantitative analysis of the pressure dependence of the intensities and by the energy-resolved spectra, which will be discussed in Secs. IV, V, and IX.

The effective formation of vdW complexes of large molecules with the heavy rare gases Ar, Kr, and Xe is a consequence of the absence of appreciable effects of velocity slip in these beams.[25] In these heavy diluents there is a proper velocity matching between the tetracene and the diluent favoring complex formation. On the other hand, in a light diluent, e.g., Ne or He, one expects an appreciable velocity slip between the tetracene and the diluent in the initial stages of the

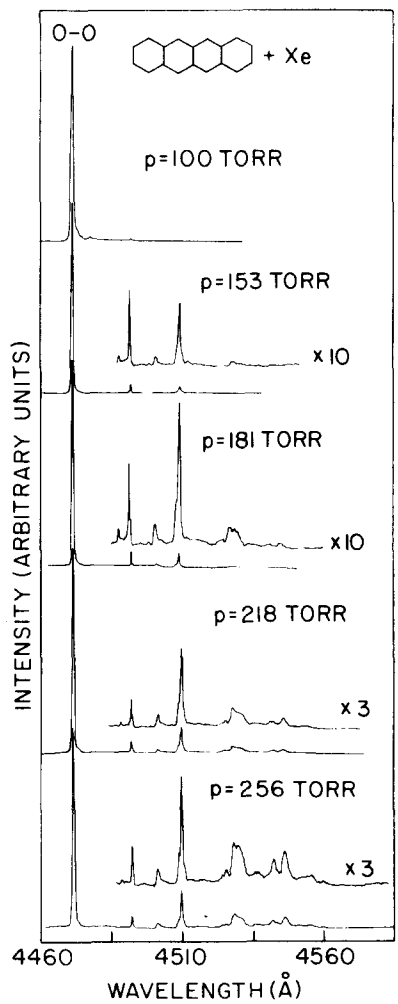

FIG. 3. Fluorescence excitation spectra of the $S_0 \rightarrow S_1$ electronic origin of tetracene and of TXe_n complexes. Tetracene (at a fixed vapor pressure of ~ 0.1 Torr) was seeded in Xe and expanded through the nozzle. All experimental conditions are as in Fig. 1. The vibrationless 0–0 excitation of bare tetracene at 4472 Å is marked 0–0. All these fluorescence excitation spectra were measured on an absolute intensity scale; the relative intensities I of the bare molecule 0–0 band are $I = 1.00$ at $p = 100$ Torr, $I = 0.50$ at $p = 153$ Torr, $I = 0.33$ at $p = 181$ Torr, $I = 0.20$ at $p = 218$ Torr, and $I = 0.10$ at $p = 256$ Torr. The fluorescence excitation spectra of the TXe_n molecules are displayed in two intensity scales, as marked on the figure.

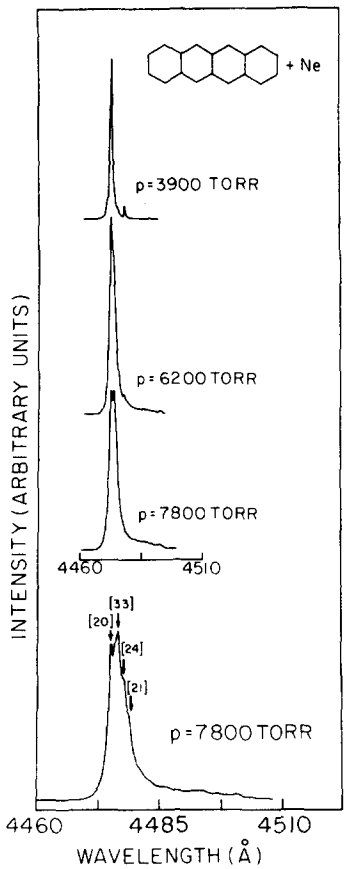

FIG. 4. Fluorescence excitation spectra of tetracene (vapor pressure of 0.1 Torr) in supersonic expansions of Ne. The pressures of Ne are indicated on the spectra. In these high-flow experiments the laser crossed the jet at 3 mm down the nozzle. At $p = 7800$ Torr a new spectral feature located at $\delta\nu = 5$ cm^{-1} towards lower energies from the 4472 Å 0–0 band of the bare tetracene molecule is observed. The lowest spectrum shows again the fluorescence excitation at $p = 7800$ Torr on an expanded (×2) wavelength scale. The numbers in square brackets [ ] represent the decay lifetimes (in nsec) of the individual spectral features.

expansion, so that complex formation will be ineffective. Only at a later stage of the expansion in a light diluent is the velocity slip reduced and three-body low-energy collisions required for complex formation can prevail. However, then the pressure is low and complex formation is ineffective. Consequently, vdW molecules between Ne and He are expected to be formed only at appreciably higher stagnation pressure than for Ar, Kr, and Xe. To demonstrate the effect of the velocity slip on the degree of vdW complexation of tetracene, we present in Fig. 4 the fluorescence excitation of tetracene seeded in Ne in high-flow supersonic expansions.[25] At $p = 3900$ Torr weak sequence bands of the isolated molecule, whose intensity is ~1% of the 0–0 transition, are still exhibited. Only at $p = 7800$ Torr additional bands, attributed to TNe with $\delta\nu = 5$ cm^{-1} and to higher (unidentified) TNe$_n$ complexes, were exhibited. Using He as a diluent, we were unable to observe any vdW complexes between He and tetracene up to $p = 8000$ Torr.

IV. FORMATION KINETICS AND SPECTROSCOPIC ASSIGNMENTS

The spectral features appearing on the low energy side of the 0–0 transition of the bare molecule were assigned to the vibrationless electronic transitions of TR$_n$ vdW molecules. The spectroscopic identification of the TR$_n$ complexes with respect to their chemical composition is of interest for several reasons. First, it is interesting to inquire whether several TR$_n$ chemical isomers with a fixed value of n but with geometrically inequivalent sites for the R atoms are energetically stable for such large vdW molecules. In this case one expects several distinct spectral features corresponding to a single chemical TR$_n$ composition. Second, low frequency vibrational structure, involving vibrational modes of the R atoms relative to the aromatic molecule, may be exhibited in the spectrum. In this case a multiple spectrum with several distinct spectral features corresponding to a single TR$_n$ molecule will be exhibited. The distinction between a multiple spectrum originating from chemical isomers or from the low frequency vibrational structure of a single vdW molecule can be ambiguous, and one has to rely on model calculations of such vibrational structure as well as on indirect arguments based on a comparison of the spectra of TR$_n$ molecules with variable coordination numbers. Third, the identification of the parentage of the individual spectral features is important for the elucidation of the effects of microscopic solvent perturbations on the energetics of electronic excitations of the large molecule. Fourth, on the basis of the identification of the parentage of the individual spectral features, one can interrogate excited-state interstate and intrastate dynamics of a photoselected excited state of a TR$_n$ molecule. Fifth, the understanding of the formation kinetics of these complexes between large aromatic molecules and rare-gas atoms is of intrinsic interest. In particular, it is intriguing to inquire whether vdW formation between T and R atoms involves a three-body collision, as is the case for vdW complexes between small molecules and rare gases, or whether a sticky TR complex characterized by a long lifetime can be produced via a two-body collision with the large molecule acting as an internal "heat bath" for the vibrational redistribution of the excess energy of the vdW bond. Sixth, the formation kinetics of such vdW molecules are relevant for the elucidation of the microscopic aspects of nucleation.

Several spectroscopic diagnostic methods were utilized for the identification and characterization of the chemical composition of various TR$_n$ complexes.

Dependence of the energies of the spectral features attributed to vdW *complexes on the identity of the rare gas*: This qualitative criterion mentioned already in Sec. III segregates the spectral features of the bare molecule from those of the vdW complexes.

Intensity conservation rule: We shall demonstrate in Sec. IV.A that the decrease in the intensity of the 0–0 transition of the bare molecule with increasing stagnation pressure is balanced by the increase in the

intensities of the spectral features attributed to the vdW complexes. This conservation rule yields a quantitative diagnostic method, which provides strong support for our general assignment of the new spectral features appearing at higher pressures to vdW complexes. In addition, the intensity conservation rule inspires confidence in our kinetic analysis of the pressure dependence of the intensity data.

Disappearance of the 0–0 *transition of the bare molecule*: The pressure dependence of the intensity of the vibrationless transition of the bare molecule T, analyzed in Sec. IV.B, provides important evidence regarding the mechanism of the formation of the TR_1 vdW molecule, which occurs via three-body collisions.

Pressure dependence of the intensity peaks of the TR_n *molecules*: The relative intensity of the peaks attributed to the TR_n vdW molecule are found to exhibit a functional dependence of the form p^{2n} on the stagnation pressure p at low values of p. At higher pressures a more complete analysis is required. Such a p^{2n} power law was used by Smalley, Levy, and Wharton[40] for the identification of HeI_2 and He_2I_2 vdW molecules. We shall utilize a slightly improved version of the p^{2n} power law for the identification of TAr_n and TKr_n complexes. The pressure dependence of the individual spectral features provides a conclusive spectroscopic method for the identification of the chemical composition of the various TR_n vdW molecules.

Order of appearance of the spectral bands: With increasing stagnation pressure spectral features of TR_n complexes with progressively higher coordination number n are expected to appear. This semiquantitative criterion is very useful for the identification of TR_n molecules.

A. Intensity conservation

In measuring the fluorescence excitation spectra of T in Ar, presented in Fig. 1, we have carefully monitored the absolute intensities of the 0–0 band of the bare molecule at different stagnation pressures of the diluent, while the partial pressure of T in the sample chamber was maintained constant. The values of the integrated intensity $A_0(p)$ of the electronic origin of T in the fluorescence excitation spectrum at the diluent pressure p are summarized in Table I. It is convenient to normalize these values of $A_0(p)$ to the value $A_0(\bar{p})$ obtained at the pressure $\bar{p}=180$ Torr of Ar, where the molecule is effectively cooled and free of vibrational sequence congestion, while the vdW complexation is still negligible. The decrease of $A_0(p)$ with increasing p is accompanied by the simultaneous increase in the integrated intensities of the low-energy spectral features, which are attributed to vdW complexes. Let us label by $A_j(p)$ the integrated intensity of the jth low-energy spectral feature in the fluorescence excitation spectrum at the pressure p. The index $j=1, 2, 3, \ldots$ is taken in order of decreasing energy of the spectral features which correspond to the (as yet unidentified) vdW molecules. Provided that the oscillator strengths and the emission quantum yields for all the vdW complexes are equal to those of the bare molecule, we would expect the intensity data to obey the simple conservation relation

$$A_0(p)+\sum_{j=1}^{\infty} A_j(p)=\text{const} \qquad \text{(IV.1)}$$

for all p.

TABLE I. Intensity conservation for the formation of tetracene–Ar complexes.

P (Torr)	$A_0(\bar{p})/A_0(p)$	$r(p)$	$q(p)$	$\ll\tau\gg/\tau_0$
180	1.00	1.12		
478	2.00	2.24	1.29	1.04
609	3.00	3.36	2.78	1.18
710	5.00	5.60	5.04	1.10
855	10.00	11.2	12.87	1.26

A more careful analysis indicates that the simple conservation rule (IV.1) does not strictly apply to the fluorescence excitation spectra we have been analyzing. Equation (IV.1) has to be corrected for the variation in the fluorescence quantum yields of the various vdW molecules. Let us denote by τ_j $(j=1, 2, \ldots)$ the experimental radiative decay lifetime of the $S_1(0)$ state of the vdW complex, which gives rise to the jth peak, while $\tau_0=19$ nsec is the lifetime of the vibrationless level of the S_1 state of the bare T molecule. The lifetimes of the various TAr_n complexes, which were already briefly reported by us[16] and which will be presented in Sec. V, vary within 50% relative to τ_0. We shall assume that the oscillator strengths and the pure radiative lifetimes of various TAr_n complexes are invariant with respect to their chemical composition, being equal to the corresponding quantities for the $S_1(0)$ state of the bare molecule. The approximate conservation law (IV.1) has to be replaced by the conservation of the integrated absorption strengths for the bare molecule and for all the vdW complexes. Let $B_0(p)$ and $B_j(p)$ be the integrated absorption strengths at pressure p of the bare molecule and of the jth vdW spectral feature, respectively. These absorption strengths are given by the products of an absorption coefficient and the number of molecules in a given TR_n complex or in the bare T composition. The conservation law can be expressed in the form

$$B_0(p)+\sum_{j=1}^{\infty} B_j(p)=\text{const} \qquad \text{(IV.2)}$$

at all p.

Next, we shall invoke the simple relations between absorption and fluorescence excitation spectra

$$A_j(p)=B_j(p)\,\tau_j/\tau_r\,, \qquad \text{(IV.3)}$$

where τ_r is the pure radiative lifetime, which is taken to be equal for the bare T molecule and for all TAr_n complexes, being in accord with our previous assumption of equality of all the oscillator strengths. Accordingly, Eqs. (IV.2) and (IV.3) result in the relation

$$A_0(p)+\sum_{j=1}^{\infty}\left(\frac{\tau_0}{\tau_j}\right)A_j(p)$$
$$=A_0(\bar{p})\left[1+\sum_{j=1}^{\infty}\left(\frac{\tau_0}{\tau_j}\right)\frac{A_j(\bar{p})}{A_0(\bar{p})}\right] . \quad \text{(IV.4)}$$

Note that Eq. (IV.4) is independent of τ_r, being determined by the lifetimes of the T and TAr_n molecules, as well as by the intensities in the fluorescence excitation spectra. Let us assume that the decay lifetime of a given class of TR_n molecules is independent of the coordination number n. For the TAr_n molecules we shall report in Sec. VIII a variation of 50% in the decay lifetimes, the value of the ratio

$$S(p)=\sum_{j=1}^{\infty}A_j(p)\Big/\sum_{j=1}^{\infty}\left(\frac{\tau_0}{\tau_j}\right)A_j(p) \quad \text{(IV.5)}$$

being $S(p)=1.20$ at $p=450$ Torr. Taking an average value $\langle\langle\tau\rangle\rangle$ for the lifetimes of the vdW complexes, the intensity conservation law can be expressed in the form

$$\langle\langle\tau\rangle\rangle/\tau_0=q(p)/[r(p)-1] , \quad \text{(IV.6)}$$

where

$$q(p)=\sum_{j=1}^{\infty}A_j(p)/A_0(p) , \quad \text{(IV.6a)}$$

$$r(p)=\eta A_0(\bar{p})/A_0(p) , \quad \text{(IV.6b)}$$

$$\eta=1+\sum_{j=1}^{\infty}\left(\frac{\tau_0}{\tau_j}\right)\frac{A_j(\bar{p})}{A_0(\bar{p})} . \quad \text{(IV.6c)}$$

In Table I we present the relative emission quantum yields from all the vdW complexes in the tetracene Ar system at different pressures. The areas $A_j(p)$ were calculated by numerical integration of the spectra of Fig. 1. The parameter η [Eq. (IV.6c)] was calculated for each diluent from the relative decrease of the amplitude of the peak of the bare molecule at the pressure $\bar{p}$ based on experimental results, which will be presented in Sec. IV.B. These parameters are $\eta=1.12$ for T–Ar, $\eta=1.24$ for T–Kr, and $\eta=1.56$ for T–Xe. From the data of Table I we conclude that the lifetimes of the TAr_n complexes are longer by ~10%–30% relative to the lifetime of the bare T molecule. This result is in complete agreement with the direct determination of the decay lifetimes presented in Sec. VIII, which reveals a lengthening of most of the lifetimes of these complexes by 10%–50%, while the quantitative weighting of the experimental lifetimes, according to relation (IV.5), results in $\langle\langle\tau\rangle\rangle/\tau_0=1.20$ at $p=450$ Torr, which is in reasonable agreement with the results of Table I. It is apparent that the intensity conservation law (IV.6) is obeyed for the tetracene–Ar system within an accuracy of ~20%. This analysis of the intensity conservation does not yet enable us to provide an identification of the vdW complexes; this goal will be accomplished on the basis of the pressure dependence of the intensities. From the analysis of the intensity conservation, two important conclusions emerge. First, these data provide compelling evidence for the validity of the assignment of the new low-energy spectral features to electronic excitation of (as yet unidentified) TAr_n vdW molecules. Second, the present analysis inspires confidence in the experimental techniques utilized by us for the controlled synthesis of these vdW molecules. We expect these techniques to be sufficiently accurate to provide quantitative kinetic information on the formation mechanism of these complexes.

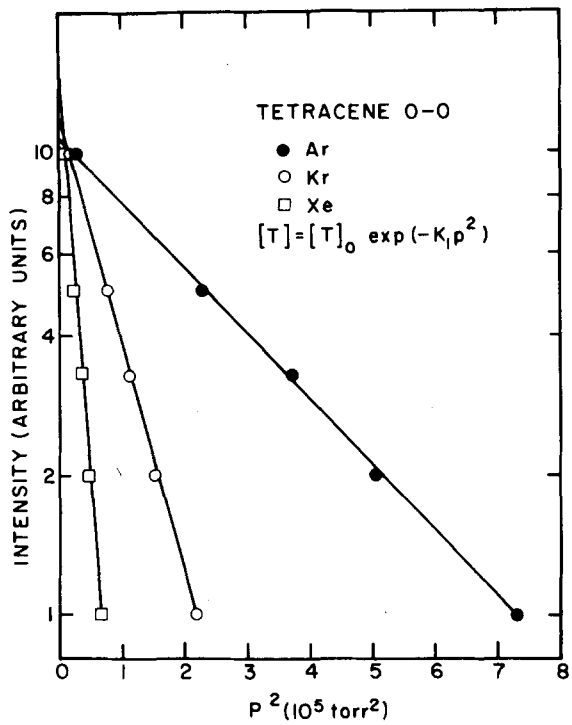

FIG. 5. The dependence of the intensity [T] of the 0–0 transition of the bare tetracene molecule on the stagnation pressure p of the rare gas. For tetracene expanded in Ar, Kr, and Xe, these data obey the relations $[T]=[T]_0\exp(-K_1p^2)$, where K_1 is a three-body recombination coefficient.

B. Kinetics of complexation of bare tetracene

When the stagnation pressure of the diluent is gradually increased, the fraction of the bare T molecule decreases due to the formation of TR_n molecules. We have followed the disappearance of the 0–0 spectral feature of the bare T molecule in supersonic expansions of Ar, Kr, and Xe by monitoring the pressure dependence of the intensity of the 0–0 bare-molecule band. Typical data, portrayed in Fig. 5, demonstrate that the intensity [T] of the bare molecule obyes the relation

$$[T]=[T]_0\exp(-K_1p^2) , \quad \text{(IV.7)}$$

where $[T]_0$ is a numerical constant, while K_1 corresponds to a three-body recombination coefficient. From this result is is apparent that the attachment of the first rare-gas atom to the large aromatic molecule proceeds via the three-body recombination process

$$T+R+R \xrightarrow{k_1} TR+R , \quad \text{(IV.8)}$$

with k_1 being the recombination rate. The three recombination parameters for tetracene in supersonic expansions of Ar, Kr, and Xe are assembled in Table II. To provide a semiquantitative treatment of these data, we shall not lean on the results of several previous calculations of chemical relaxation, but rather

TABLE II. Three-body recombination coefficients between tetracene and rare gases in supersonic expansions ($D = 150\ \mu$ nozzle, temperature = 493 °K).

Diluent	K_1 (atm^{-2})	σ_0 (Relative values)
Ar	2.0	1.00
Kr	6.9	1.63
Xe	25.6	2.77

consider a simple one-dimensional calculation of the recombination process accounting for the density and temperature profile of the supersonic expansion.[41] We consider the change of the concentration $T(z)$ of tetracene at the point z down the nozzle, where the velocity is $u(z)$, the sound velocity is $V_s(z)$, and the Mach number is M.

The chemical rate is

$$\frac{\partial T(z)}{\partial t} = u(z)\frac{\partial T(z)}{\partial z} = MV_s(z)\frac{\partial T(z)}{\partial z} \ . \qquad \text{(IV.9)}$$

For the three-body recombination process we have

$$\partial T(z)/\partial t = k_1(z)\rho(z)^2 T(z) \ , \qquad \text{(IV.10)}$$

where $\rho(z)$ is the local diluent density at point z, while $k_1(z)$ is the three-body recombination rate constant at this point. Utilizing the results for a free-jet expansion of a chemically inert gas, one can specify $\rho(z)$ and $V_s(z)$ in terms of their dependence on the Mach number. In a similar way, once the temperature dependence of $k(z)$ is specified the recombination rate can also be characterized by the Mach number M. From Eqs. (IV.9) and (IV.10) one obtains

$$-\frac{\partial \ln T(z)}{\partial z} = \frac{k_1(z)\rho(z)}{MV_s(z)} \ . \qquad \text{(IV.11)}$$

Integration of Eq. (IV.11) results in an explicit relation for the concentration of tetracene [T] at the interrogation point at the end of the expansion

$$[\mathrm{T}] = [\mathrm{T}]_0 \exp[-K_1\rho(0)^2] \ , \qquad \text{(IV.12)}$$

where $[\mathrm{T}]_0$ is the tetracene concentration at the nozzle. The three-body recombination coefficient appearing in Eq. (IV.12) is

$$K_1 = \frac{k_1(0)}{V_s(0)} \int_{M_1}^{M_t} \left[\frac{\rho(M)}{\rho(0)}\right]^2 \left[\frac{V_s(0)}{V_s(M)}\right]\left[\frac{k_1(M)}{k_1(0)}\right] \frac{dM}{M(dM/dz)} \ , \qquad \text{(IV.13)}$$

where $k_1(0)$, $V_s(0)$, and $\rho(0)$ represent the three-body recombination rate, the sound velocity, and the density at the nozzle, respectively, and where supersaturation has occurred. M_1 is the Mach number at supersaturation, while M_t represents the terminal Mach number.

Confronting Eq. (IV.12) with the experimental relation (IV.7) results in an explicit expression for the three-body recombination rate in terms of Eq. (IV.13). Assuming that the lower limit M_1 of this integral is independent of the nature of the diluent, we can assert that these recombination rates in different diluents are essentially determined by the values of $k_1(0)$. We did not succeed in accounting for the experimental values of K_1 in terms of the "soft sphere" model[42] for three-body collisions, as the one order of magnitude increase of the relative values of $k_1(0)$ (Table II), going from Ar to Xe, is much more pronounced than predicted on the basis of the increase of the strength of the attractive vdW interaction[43] for T–Xe as compared to T–Ar. A plausible reason for this failure may be due to the inherent limitations of the soft sphere model[42] in accounting for three-body recombination of a rare gas with a large aromatic molecule. Invoking an alternative empirical approach to characterize the kinetic data, we set[42] $k_1(0) = P\tilde{K}z$, where $P \sim 1$ is the complex stabilization probability. z is the rate of collisions of TR with a third body $z = \pi\bar{v}\sigma_0$, where $\bar{v}$ is the mean velocity and σ_0 is the cross section for two-body collisions. $\tilde{K}$ is the equilibrium constant[42] $\tilde{K} \propto \sigma_0^{3/2}$. Accordingly, $k_1(0) \propto \sigma_0^{5/2}$.

C. Pressure dependence of the spectral intensities of TR_n molecules

The quantitative features of the complexation kinetics of the bare T molecule in supersonic expansions of Ar, Kr, and Xe clearly demonstrate that the TR_1 vdW complex between tetracene and a single rare-gas atom is produced via a three-body collision, according to Eq. (IV.8). On the basis of this observation we can provide an unambiguous identification of the spectral features which correspond to the 0–0 transition of the TAr_1, TKr_1, and TXe_1 molecules, whose absorption intensities are expected to be proportional to p^2. We have already analyzed[16] the pressure dependence of the highest energy pronounced spectral feature of vdW molecules of tetracene with Ar, Kr, and Xe, which are located at the following energies $\delta\nu$ below the electronic origins of the bare molecule: $\delta\nu = 35\ cm^{-1}$ for Ar, $\delta\nu = 70\ cm^{-1}$ for Kr, and $\delta\nu = 101\ cm^{-1}$ for Xe. The relative intensity of these three spectral features, being normalized to the intensity [T] of the bare molecule, exhibits[16] a p^2 pressure dependence, providing spectroscopic identification of the TR_1 (R = Ar, Kr, and Xe) molecule. To identify the high TR_n complexes we shall invoke a basic working hypothesis, asserting that the formation mechanism of all TR_n complexes involves a three-body collision

$$TR_{n-1} + R + R \xrightarrow{k_n} TR_n + R \ , \qquad \text{(IV.14)}$$

where k_n is the three-body rate constant for the formation of the TR_n molecule. These rate constants k_n depend on the local temperature, local density, and relative velocities of TR_{n-1} and R in the supersonic expansion. It should be emphazied that the mechanistic assumption concerning three-body recombination of large aromatic molecules with rare gases is by no means self-evident. The assumption inherent in Eq. (IV.14) is that the density of vibrational levels of the large aromatic molecule in the vicinity of the dissociation energy of the T–R bond is sufficiently low, whereupon sticky T + R two-body collisions, where the excess energy is

effectively redistributed in the large molecules, are inefficient in stabilizing the complexes. The justification of this basic assumption will be provided on the basis of the experimental data.

The local concentrations $TR_n(z)$ of the complexes at the position z can now be readily expressed using the one-dimensional description of the supersonic expansion

$$\partial TR_n(z)/\partial z = [k_n(0) f_n(z) TR_{n-1}(z) - k_{n+1}(0) f_{n+1}(z) TR_n(z)] \rho(0)^2 , \quad \text{(IV.15)}$$

where $k_n(0)$ is the three-body recombination rate at the nozzle and the diluent density is $\rho(0)$. $f_n(z)$ is a correction function accounting for the velocity, temperature, and density profiles in the expansion. For the simple model already used in Sec. IV.B,

$$f_n(z) \equiv f_n(M) = \frac{1}{MV_s(0)} \left[\frac{\rho(M)}{\rho(0)}\right]^2 \left[\frac{V_s(0)}{V_s(M)}\right] \frac{k_n(M)}{k_n(0)} . \quad \text{(IV.16)}$$

For the sake of a semiquantitative treatment of the pressure dependence of the abundance of TR_n molecules, we shall at this stage invoke a simplifying assumption asserting that the three-body rate constants $k_n(0)$ are independent of n. This assumption will be relaxed in Sec. IV.D.

The democratic assumption now implies that the local rates $k_n(0) f_n(z)$ are independent of n. Accordingly, we can define a simple three-body formation coefficient

$$K = k(0) \int_{M_1}^{M_t} f(M)\, dM/(dM/dz) \quad \text{(IV.17)}$$

for the system. The kinetic equations (IV.15) are now analytically soluble, resulting in concentrations $TR_n(z_\infty)$ of the complex in the interrogation area at the point z_∞:

$$TR_n(z_\infty) = T(0) P(n) , \quad \text{(IV.18)}$$

where the distribution $P(n)$ of the TR_n molecule is Poissonian

$$P(n) = \exp(-Kp^2)[(Kp^2)^n/n!] , \quad \text{(IV.19)}$$

with K being given by Eq. (IV.17). The parameter specifying the distribution is Kp^2, the mean value $\langle n \rangle$ of the complex size is given by

$$\langle n \rangle = \sum_{n=0}^{\infty} nP(n) = Kp^2 , \quad \text{(IV.20a)}$$

while the spread (variance) of the distribution is

$$\sigma_n = (\langle n^2 \rangle - \langle n \rangle)^{1/2} = K^{1/2} p . \quad \text{(IV.20b)}$$

To make contact with the experimental data we identify $P(n)$ (apart from irrelevant numerical factors) with the spectral intensity $[TR_n]$ of the TR_n molecule, while $\exp(-Kp^2)$ can be identified, according to Eqs. (IV.7) and (IV.12), with the intensity $[T]$ of the bare molecule. Consequently, Eq. (IV.19) is

$$\frac{[TR_n]}{[T]} = (Kp^2)^n . \quad \text{(IV.21)}$$

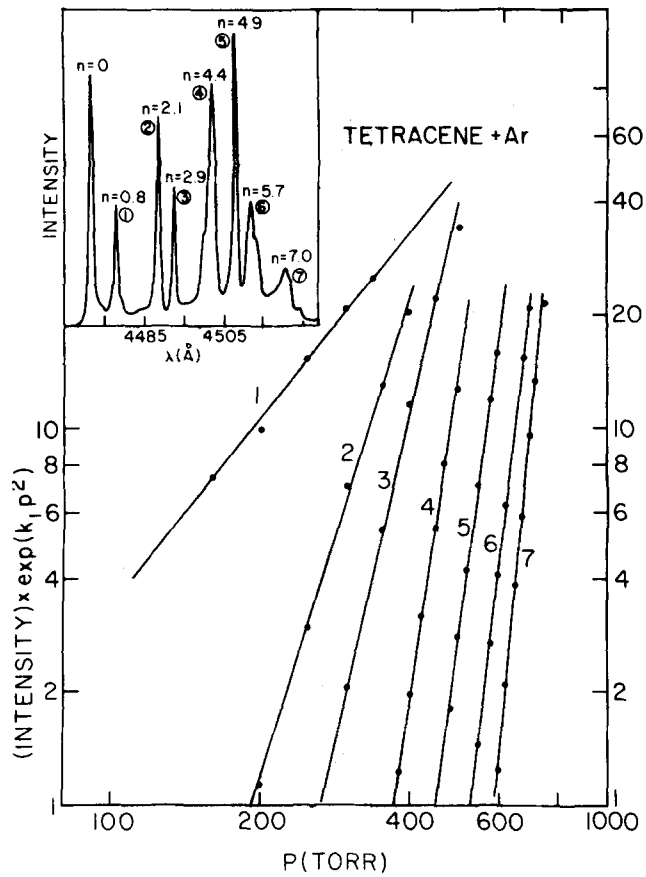

FIG. 6. The dependence on the Ar pressure of the normalized intensities $[TAr_n]/[T]$ of the spectral features of the TAr_n molecules normalized by the intensity of the bare molecule for supersonic expansions of tetracene in Ar. The upper insert shows the fluorescence excitation spectrum of tetracene seeded in Ar expanded at $p = 710$ Torr. The individual spectral features are labeled by the indices $j = 1, 2, \ldots, 7$ in order of increasing wavelength. The pressure dependence of the normalized intensities of these spectral features is of the form p^{2n}. The values of n obtained from this analysis are shown in the spectrum (upper insert).

Thus, the spectral intensity of the TR_n complex normalized to the intensity of the bare molecule is proportional to p^{2n}. This p^{2n} power law was applied by us for the identification of the TAr_n and TKr_n complexes.

We have analyzed the spectral features appearing on the low-energy side of the bare molecule 0–0 vibrationless transition for the pressure range $p = 180$–853 Torr in Ar and for $p = 135$–465 Torr in Kr in terms of Eq. (IV.21). To do so we plotted the pressure dependence of the intensity ratio $[TR_n]/[T] = \exp(Kp^2)[TR_n]$, where the three-body recombination coefficients K for Ar and Kr are taken from the slopes of the lines in Fig. 5. In the spectra of the T–Ar_1 system (Fig. 6) we were able to identify seven distinct spectral features (see the insert in Fig. 6) which are labeled by the numbers $j = 1, 2, \ldots, 7$ in the order of decreasing energy. As is evident from Fig. 6, the relative peak intensities of these seven spectral features exhibit the p^{2n} dependence in order of decreasing energy. The

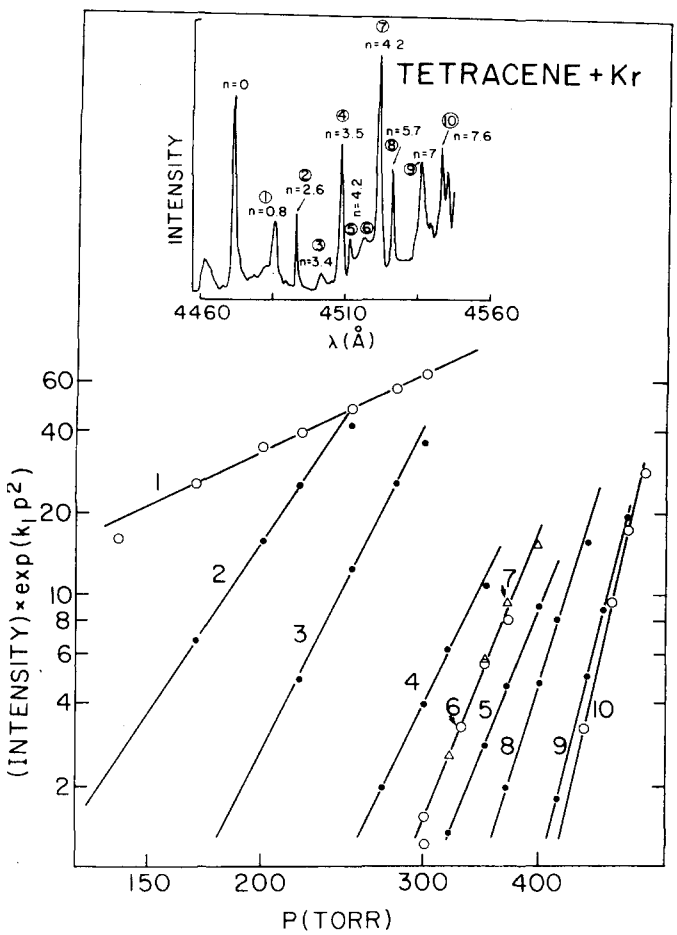

FIG. 7. The dependence on the Kr pressure of the normalized intensities $[TKr_n]/[T]$ of the spectral features of TKr_n molecules normalized by the intensity of the bare molecule for supersonic expansions of tetracene in Kr. The upper insert shows the fluorescence excitation spectrum of tetracene seeded in Kr expanded at $p = 465$ Torr. The individual spectral features are labeled by the indices $j = 1, \ldots, 10$ in order of increasing wavelength. The pressure dependence of the normalized intensities of these spectral features is of the form p^{2n}. The values of n obtained from this analysis are shown on the spectrum (upper insert).

values of n, obtained from plots according to Eq. (IV.21), are presented in Fig. 6, being very close to the integers $n = 1, 2, \ldots, 7$. These data provide spectroscopic identification of the seven peaks in the T–Ar system, corresponding to the TAr_n molecules with the composition $n = 1, 2, \ldots, 7$. In the T–Ar system there is essentially a single spectral feature which can be attributed to a given TAr_n chemical composition and no multiple peaks corresponding to a fixed value of n were experimentally observed. Next, we proceed to the analysis of the spectra of T–Kr complexes, which are somewhat more complicated. In the spectra of T–Kr we have identified ten distinct spectral features (see the insert in Fig. 7) which are labeled by $j = 1, 2, \ldots, 10$ in order of decreasing energy. In this system there is a considerable intensity alternation, e.g., while the $j = 1$, 2, 4, and 7 peaks are strong, the $j = 3$, 5, and 6 peaks are weak. The values of n for the T–Kr system obtained from the linear plots implied by the p^{2n} power law (see Fig. 7) are summarized in the insert in Fig. 7. On the basis of these results the $j = 1$ peak is assigned to TKr_1, the $j = 2$ peak is attributed to TKr_2, the weak $j = 3$ and the strong $j = 4$ peaks are both assigned to TKr_3, while the two weak $j = 5$ and 6 peaks, together with the intense $j = 7$ peak, are all attributed to TKr_4. Thus, for the TKr_n complexes there are no multiple peaks corresponding to $n = 1$ and 2; however, for $n = 3$ and 4 there are several spectral peaks corresponding to a fixed chemical composition of the complex.

On the basis of the pressure dependence of the intensities of the spectral features of T–Ar and T–Kr, appearing on the low energy side of the 0–0 transition of the bare T molecule, we were able to provide spectroscopic identification of TAr_n ($n = 1, \ldots, 7$) and TKr_n ($n = 1, \ldots, 4$) molecules. As these spectral features for each TR_n with fixed n correspond to the lowest energy excitation of the vdW molecule, they can safely be assigned to 0–0 excitations of the vdW complexes. Supplementary and complementary information concerning the identity of the vdW molecules between T and rare gases, as well as between T and other molecules, can be obtained from an analysis of the order of appearance of the spectral features corresponding to vdW molecules, which will now be considered.

D. Order of appearance of the TR_n molecules

According to the three-body formation mechanism [Eq. (IV.14)], one expects that with a gradual increase of the stagnation pressure, the order of appearance of the spectral features attributed to TR_n molecules will be sequential starting from $n = 1$ at moderate values of p. We have conducted a detailed analysis of the T–Ar system in the context of the order of appearance of the spectral features in the low energy side of the electronic origin of the bare molecule. In Fig. 8 we portray the pressure dependence of the relative absorption intensities of eight individual spectral features in the T–Ar system, which correspond to the bare molecule ($n = 0$) and to the lowest seven ($n = 1, 2, \ldots, 7$) complexes. These relative (absorption) intensities b_n are given by

$$b_n = \left(\frac{A_n}{\tau_n}\right) \Big/ \sum_{n=0}^{7} \left(\frac{A_n}{\tau_n}\right) , \quad n = 0, \ldots, 7 , \qquad \text{(IV.22)}$$

where A_n is the area (in arbitrary units) of the spectral feature assigned to the TAr_n molecule in the fluorescence excitation spectrum, while τ_n is the experimental decay lifetime of this spectral feature which is reported in Sec. VIII. Figure 8 provides an overview of the pressure dependence of the absorption intensities of TAr_n complexes. Without alluding to any quantitative estimates it is apparent that the spectral features corresponding to the low TAr_1 and TAr_2 complexes can safely be assigned from a cursory examination of the order of appearance of the vdW molecules.

To provide a more elaborate treatment of the order of appearance of the TAr_n complexes, we have solved numerically the set of eight kinetic equations (IV.15). The correction function $f_n(z)$ was taken to be independent

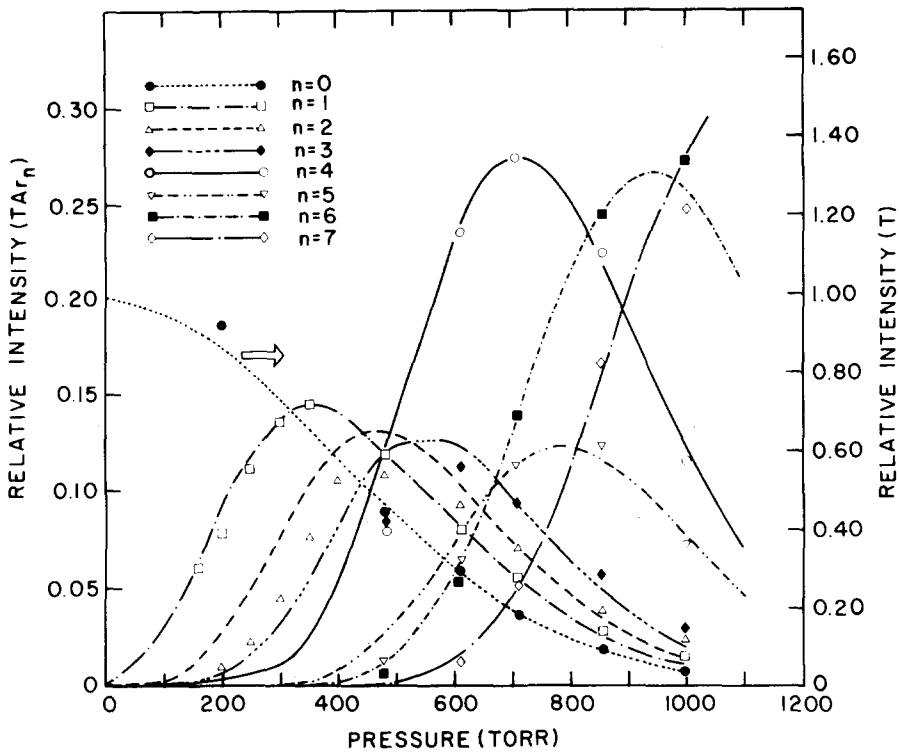

FIG. 8. The pressure dependence of the relative (absorption) intensities [Eq. (IV.22)] of T and of TAr_n ($n=1,\ldots,7$) in the tetracene–Ar supersonic expansions. The labeling of the experimental data points for the various molecules is indicated on the figure. The eight solid curves for the T molecule and the seven TR_n ($n=1,\ldots,7$) molecules were calculated by numerical integration of the one-dimensional differential equation for three-body complexation in the supersonic expansion, as described in the text. The required eight three-body rate constants were fit from the experimental data at $p=710$ Torr.

of n, i.e., $f_n(z)=f(z)$ for all values of n, and is taken in the simple functional form $f(z)=[D/(z+z_0)]^2$. Here, D is the nozzle diameter and $z_0=2D-4D$ represents a characteristic distance where supersaturation occurs. This admittedly crude form of $f(z)$ is intended to mimic the density profile in the supersonic expansion, which approaches the proper asymptotic value of $(D/z)^2$. However, the unknown temperature dependence of the three-body recombination rate and the effect of the velocity profile were not incorporated. The differential equations (IV.15) were integrated for the populations of the TR_n molecules ($n=0,\ldots,7$) at $z=50D$. We have used the experimental data at a single pressure ($p=710$ Torr) to fit the eight three-body rate constants, which in arbitrary units are given by $k_1(0)=1.00$, $k_2(0)=4.5$, $k_3(0)=4.4$, $k_4(0)=4.0$, $k_5(0)=1.5$, $k_6(0)=2.9$, $k_7(0)=1.2$, and $k_8(0)=0.8$. These rates were subsequently used to provide the pressure dependence of the populations of the TR_n molecules over the entire pressure range (Fig. 8), yielding a reasonable account of the experimental data. In view of our crude analysis we did not attempt to refine the eight parameter fit of the 60 experimental data points of Fig. 8. Nevertheless, in spite of our simplistic approach, two conclusions emerge from the present analysis concerning the T–Ar system. First, additional support is provided for the three-body formation mechanism of the TAr_n complexes. Second, the variation of the relative rates $k_n(0)$ over the range 1.0–4.0 is rather irregular and no further systemization of the microscopic rates was attempted.

The order of appearance of the spectral features of the individual TR_n molecules with increasing pressure provides a semiquantitative diagnostic method for the identification of the chemical composition of these complexes. We have utilized this diagnostic method for the assignment of the absorption features of the TXe_n complexes. In the spectra of the T–Xe system (Fig. 3) the strong spectral feature located at $\delta\nu=101$ cm^{-1} to lower energies from the bare molecule electronic origin as well as the weak band at $\delta\nu=83$ cm^{-1} exhibit an identical pressure dependence of the form given by Eq. (IV.21) with $n=1.3\pm0.4$, and are assigned to TXe_1. Next in order of appearance are the strong spectral feature at $\delta\nu=189$ cm^{-1} and the weak feature at $\delta\nu=147$ cm^{-1}, both of which reveal an identical pressure dependence of the form given by Eq. (IV.21) with $n=2.2\pm0.4$, and which are attributed to TXe_2. This preliminary assignment of the spectral features of TXe_n complexes is portrayed in Fig. 9.

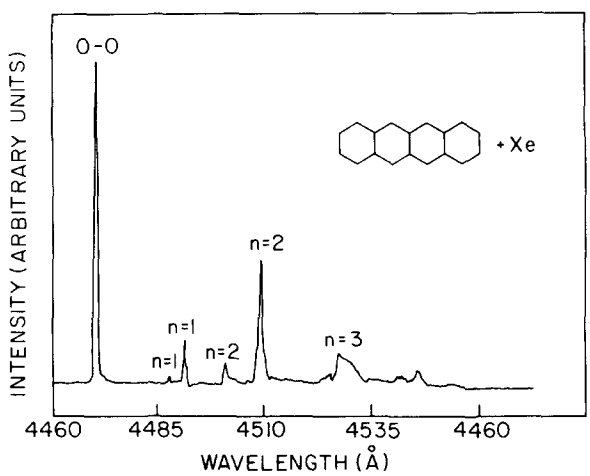

FIG. 9. A preliminary assignment of the spectral features of TXe_n molecules on the basis of their order of appearance.

TABLE III. Excited-state energetics of the vibrationless excitation of the TR_n molecule.

Molecules	Band number j	λ^a (Å)	Coordination number n^b	$\delta\nu^c$ (cm^{-1})
TAr_n	0	4471.5	0	0
	1	4478.5	1	35
	2	4489.3	2	88
	3	4493.4	3	109
	4	4502.8	4	155
	5	4508.6	5	184
	6	4512.7	6	204
	7	4521.2	7	246
TKr_n	0	4471.5	0	0
	1	4485.6	1	70
	2	4493.5	2	110
	3	4501.8	3 (weak)	150
	4	4509.1	3	186
	5	4511.9	4 (weak)	200
	6	4516.3	4 (weak)	223
	7	4521.6	4	248
	8	4526.3		271
	9	4535.7		317
	10	4542.7		350
TXe_n	0	4471.5	0	0
	1	4488.2	1 (weak)	83
	2	4491.8	1	101
	3	4501.0	2 (weak)	147
	4	4509.5	2	189
	5	4525.0	(broad)	265
	6	4528.0	(broad)	278
	7	4542.0	(broad)	347
	8	4546.0	(broad)	368

[a]Absolute accuracy ±2 Å. Relative accuracy ± 0.3 Å.
[b]From analysis in Figs. 6–8.
[c]Red shift of vibrationless excitation of TR_n from the electronic origin of T. Accuracy of $\delta\nu$ data is ±2 cm^{-1}.

The quantitative analysis of the formation kinetics of the TR_1 (R = Ar, Kr, and Xe) molecules presented in Sec. IV.B together with the semiquantitative analysis of the formation of higher TR_n (R = Ar, Kr, and Xe) molecules presented in Secs. IV.C and IV.D provide *a posteriori* justification for our basic assumption that such vdW molecules between a large aromatic, e.g., tetracene and rare-gas atoms, are produced via a three-body collision. This observation clearly rules out the formation of stable "sticky" complexes via two-body collisions between rare-gas atoms and large aromatic molecules, which subsequently can exhibit intramolecular vibrational energy flow. This negative result is not entirely surprising as the density of vibrational states of such a complex is rather low, at least for vdW complexes of large molecules with a moderately small number of rare-gas atoms. For these large vdW molecules the three-body production mechanism prevails, as is the case for the formation of vdW molecules of diatomic iodine with rare-gas atoms.[13–15]

V. EXCITED-STATE ENERGETICS OF TR_n MOLECULES

The spectroscopic studies of the formation kinetics of the TR_n lead to two major results. First, we were able to identify vdW molecules of tetracene characterized by the chemical composition TAr_n ($n = 1, \ldots, 7$), TKr_n ($n = 1, \ldots, 4$), and TXe_n ($n = 1, 2$). Second, we were able to assign the individual spectral features which correspond to the vibrationless 0–0 electronic excitations of these TR_n molecules into their first excited singlet state. In Table III we summarize the peak energies of the spectral features attributed to the $S_0(0) \rightarrow S_1(0)$ excitations of the TR_n molecules. We shall now proceed to discuss some of the consequences of the spectroscopic identification of these complexes and subsequently we shall consider the nature of the spectral shifts.

A. Some information regarding chemical isomers and vibrational structure

From the spectroscopic identification of the TR_n molecules, the following conclusions emerge:

(1) For TAr_n ($n = 1, 2, 3$) and for TKr_1 and TKr_2 we have observed a single distinct spectral feature for each of the vdW molecules. The spectroscopic data seem to rule out the possibility of the existence of isomers, corresponding to a fixed chemical composition and different unequivalent trapping sites for these five vdW molecules. This observation concurs with the results of recent model calculations by Ondrechen

et al.[43] on the energetic stability and structure of tetracene–rare-gas complexes, which show that only a single equilibrium configuration of the TR_1 molecule and the TR_2 molecule (R = Ar, Kr, and Xe) is expected to be energetically stable.

(2) For TKr_3 and TKr_4 a multiple spectrum corresponding to each chemical composition is exhibited. There are two spectral features which correspond to TKr_3 consisting of an intense band at $\delta\nu = 186$ cm^{-1} and a weak band at $\delta\nu = 150$ cm^{-1}. Three bands were assigned to vdW molecules of the composition TKr_4, consisting of an intense band at $\delta\nu = 248$ cm^{-1} and two weak bands at $\delta\nu = 200$ and 223 cm^{-1}. This multiplet structure can originate either from the vibrational structure of a single chemical species or, alternatively, from chemical isomers. At present, an unambiguous interpretation of this multiplet structure cannot be provided. As no multiplet structure was observed for TKr_1 and TKr_2, we can safely assert that these two complexes do not reveal an analogous vibrational structure. It is rather difficult to understand why a vibrational structure with a frequency of ~25–36 cm^{-1} will be shown by TKr_3 and TKr_4 and not by TKr_1 or TKr_2. We thus tentatively assign the multiplet structures of TKr_3 and TKr_4 to chemical isomers. The model calculations of Ondrechen *et al.*[43] point towards the possibility of the existence of two chemical isomers of TKr_3, whose ground-state energies are very close.

(3) For each of the tetracene–xenon complexes TXe_1 and TXe_2, we have observed a multiplet structure consisting of a strong spectral feature and a low-energy weak band. The splittings between the strong and weak bands are 18 cm^{-1} for TXe_1 and 42 cm^{-1} for TXe_2. In view of the large spectral shifts of the TXe_1 complex relative to the bare tetracene and the large spectral shift between TXe_2 and TXe_1, the spectra of these complexes are not complicated by overlap of spectral features corresponding to different TXe_n molecules, so that more spectroscopic details are unveiled. As recent model calculations by Ondrechen *et al.*[43] on the stability of TR_n complexes indicate that only a single isomer of TXe_1 and TXe_2 is energetically stable, we are inclined to attribute the multiplet structure of these xenon complexes to vibrational structure.

B. Spectral shifts

The identification of the spectral features which correspond to well-characterized TR_n vdW complexes provides a powerful means for the exploration of the effects of weak intermolecular interactions on excited-state energetics of a large molecule. The spectral shift between the 0–0 excitation energy of an individual, well-defined, TR_n molecule and the 0–0 electronic origin of the bare tetracene molecule yields direct information on the perturbations excited by rare-gas atoms on the electronic excitation energy of the large aromatic molecule. These spectral shifts can be viewed as medium perturbations on the electronic excitations of the large molecule in a well-defined solvent environment of rare-gas atoms. These spectroscopic data bear on the consequences of solvent–solute interactions and on the role

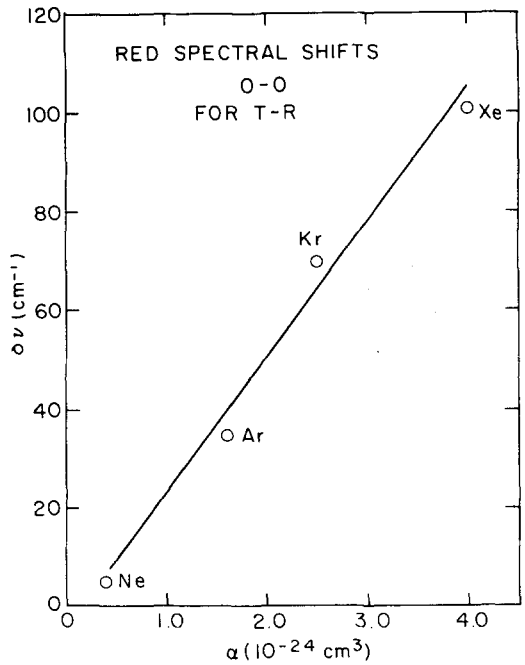

FIG. 10. The dependence of the red spectral shifts $\delta\nu$ of the vibrationless $S_0 \rightarrow S_1$ excitations of TR_1 (R = Ne, Ar, Kr, and Xe) molecules on the polarizability of the rare-gas atom.

of local solvent structure on the energetic spectral solvent shifts as viewed from the microscopic point of view. The quantitative data for the spectral shifts are summarized in Table III. These spectral shifts represent the effect of tetracene–rare-gas interactions on the energy of the vibrationless S_1 state relative to the vibrationless S_0 state. The following features of the microscopic spectral shifts are of interest:

(1) The spectral shifts induced by Ne, Ar, Kr, and Xe atoms are all towards lower energies. Such red spectral shifts are conventionally assigned[1–3] to the dominating role of dispersive interactions in modifying the energy levels. In general, the spectral shift on electronic excitation originates from the following effects: (a) electronic interactions, which involve (1) the modifications of the short-range repulsive interactions giving rise to a blue spectral shift and (2) a change in the dispersive interactions which usually result in a red spectral shift,[1] (b) effects on nuclear motion, which are (1) modifications of the difference in the zero-point energy of the large molecule between its S_1 and S_0 states and (2) the change in the zero-point energy of the vdW bonds between S_1 and S_0 states. We expect that the effects of nuclear motion are small. Furthermore, for an intravalent $\pi \rightarrow \pi^*$ excitation of the tetracene molecule we expect the changes in short-range repulsive interactions to be small. Thus, the spectral shift exerted by Ne, Ar, Kr, and Xe is expected to be dominant by dispersive effects.

(2) The microscopic spectral shifts exerted by a single rare-gas atom reveal a linear dependence on the polarizability of the perturbing atom. This is evident from Fig. 10, where we display the dependence of the red spectral shifts of the TR_1 (R = Ne, Ar, Kr, and Xe)

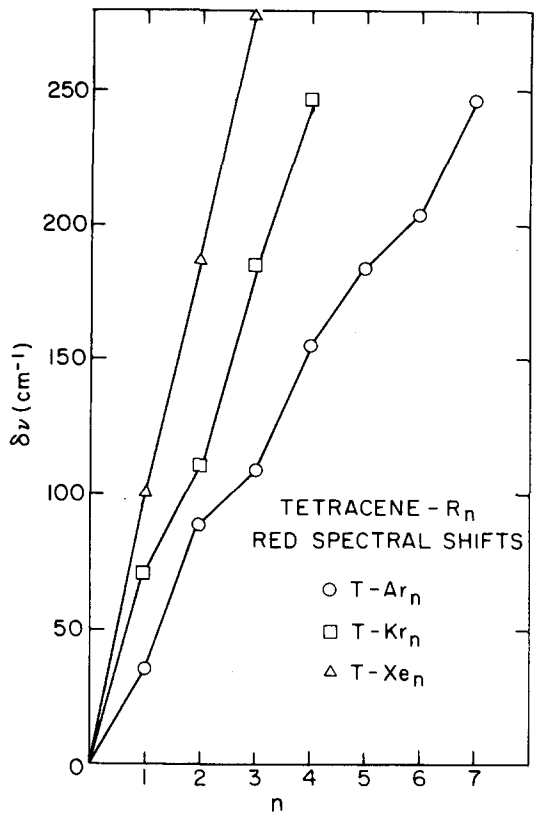

FIG. 11. The dependence of the red spectral shifts $\delta\nu$ of the vibrationless $S_0 \rightarrow S_1$ excitations of the TR_n (R = Ar, Kr, and Xe) molecules on the coordination number n. Accuracy of data points is to ± 2 cm^{-1}. The experimental points were combined by straight lines just to provide a visual demonstration of the deviations from the additivity law per added atom.

molecules on the polarizability of the rare-gas atom. This result is in accord with the general characteristics of electronic spectral shifts induced by dispersive interactions.[1] Although the theory of spectral shifts[1-3] is inapplicable to the tetracene–rare-gas systems, as the large molecule cannot be treated as a point dipole, a slightly extended version of the theory of dispersive spectral shifts[44] retains the same results regarding the linear dependence of the red shift on the polarizability of the perturber atom.

(3) The spectral shifts of the TR_n molecules are not additive per added atom, i.e., they do not obey the relation

$$\delta\nu(n) = n\delta\nu(1) , \qquad (V.1)$$

where $\delta\nu(n)$ and $\delta\nu(1)$ correspond to the spectral shifts of TR_n and TR_1, respectively. We shall refer to relation (V.1) as the additivity law per atom (ALPA) for the spectral shifts. As is evident from Fig. 11, the deviations of our spectral shifts from the ALPA are about 30%. The violation of the ALPA for the spectral shifts of the vdW complexes containing a large aromatic molecule is in contrast with the additivity law reported for the spectral shifts of vdW complexes of I_2[14,17] and tetrazine.[14] The violation of the ALPA in large TR_n molecules can originate from two causes. First, three-body interactions may be important for the excited-state energetics of such complexes. Although numerical estimates of these effects have not yet been performed, we note that in the tetrazine–Ar system[14] such three-body effects seem not to prevail. Second, the deviation of the spectral shifts for the large TR_n from the ALPA may originate from the occupation of geometrically inequivalent sites by the rare-gas atoms. While the contributions of the individual rare-gas atoms to the spectral shift are still strictly additive in a second-order treatment of the dispersive interactions, each atom yields a different contribution. We prefer this interpretation of the violation of the ALPA as it provides an overall self-consistent picture of the qualitatively different pattern of the spectral shifts of TR_n molecules studied herein and of the I_2–R_n molecules and tetrazine–R molecules studied by the Chicago group.[14,17] While for IR_n and for tetrazine–R complexes the R atoms seem to occupy geometrically equivalent sites and thus obey the additivity law, in the case of TR_n complexes the R atoms can occupy geometrically inequivalent sites on the surface of the large aromatic molecule, resulting in violation of the ALPA.

(4) The notion of violation of the ALPA due to occupation of geometrically inequivalent sites provides some indirect information on the geometry of tetracene–rare-gas complexes. Consider, for example, a TR_2 complex. The ALPA for spectral shifts would be obeyed provided that the two R atoms are located on opposite sides of the aromatic ring, each occupying the same site as the TR_1 molecule. From the experimental observation (Table III) for both tetracene–argon and tetracene–krypton complexes $[\delta\nu(2) \neq 2\delta(1)]$ we can deduce that in the energetically favorable ground-state configuration of TAr_2 and TKr_2 the two rare-gas atoms are located on the same side of the aromatic ring. This expectation is borne out by the numerical calculations of Ondrechen *et al.*[43] In a similar manner we note (Table III) that, for the main peak of the TAr_3 tetracene–argon complex, $\delta\nu(3) \neq \delta\nu(1) + 2\delta\nu(2)$, so that it is likely that the equilibrium configuration of TAr_3 does not involve a "sandwich-type" structure with two Ar atoms on one side and the third Ar atom on the other side of the aromatic ring, but rather all three Ar atoms are located on the same side of the aromatic ring.

The additivity law per added solvent atom for spectral shifts is expected to be obeyed provided that two conditions are satisfied. First, the spectral shifts can be handled by second-order perturbation theory and are additive. Second, the "solvent" atoms occupy geometrically equivalent sites. From the analysis of the effects of microscopic solvation on the excited-state energetics of the tetracene molecule, it appears that the second condition is not satisfied, resulting in the violation of the additivity law (per added solvent atom). Future theoretical studies of solvent effects on excited-state energetics of simple systems, e.g., nonpolar solute in nonpolar solvents, will have to consider the effect of inequivalent sites of the solvent in the first coordination layer.

VI. van der WAALS MOLECULES OF TETRACENE WITH OTHER SOLUTES

We have been concerned with the vibrationless $S_0 \rightarrow S_1$ transition of vdW molecules of tetracene with rare-gas atoms, interrogating the microscopic effects of "solvent–solute" interactions on excited-state energetics of a large "solute" molecule. To demonstrate the universality of these phenomena we have shown that vdW molecules of large aromatics are formed with a variety of solvent molecules which include diatomics as well as polyatomic molecules. In particular, we have investigated the spectroscopy of vdW molecules of tetracene with molecular nitrogen and have proceeded subsequently to a preliminary study of vdW complexes of tetracene with water, which are of particular interest, as well as of tetracene with another medium-sized aromatic molecule, such as benzene.

In Fig. 12 we present the fluorescence excitation spectra of tetracene expanded in N_2 in the vicinity of the electronic origin. The cooling of the internal degrees of freedom of the large tetracene molecule seeded in N_2 was less efficient than in Ar and even at $p = 450$ Torr the tetracene spectrum (Fig. 12) is still not free from vibrational sequence congestion effects. The $T(N_2)_n$ vdW molecules could be observed at the low energy side of the 0–0 of the bare molecules only at high pressures $p \geq 2$ atm. From the order of appearance of these bands we were able to assign the spectral features to specific $T(N_2)_n$ molecules (Fig. 13). We note that the spectral features assigned to those complexes containing an odd number of N_2 molecules, i.e., $T(N_2)_1$ and $T(N_2)_3$, are broad, hiding some unresolved structure, which may be due to chemical isomers. However, at present the data are insufficient for a definite identification.

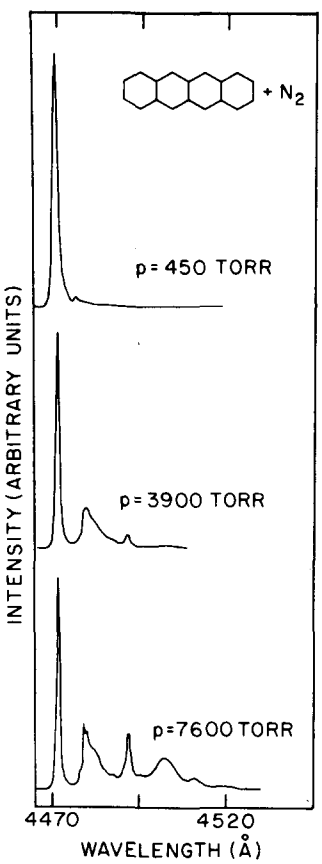

FIG. 12. Fluorescence excitation spectra of supersonic expansions (through a 150 μ nozzle) of tetracene (0.1 Torr) seeded into N_2. The N_2 pressures are indicated on the figure. In high-flow experiments at $p = 3500$ and 7600 Torr the laser crossed the jet at $X = 3$ mm down the nozzle, while for $p = 450$ Torr, $X = 7$ mm.

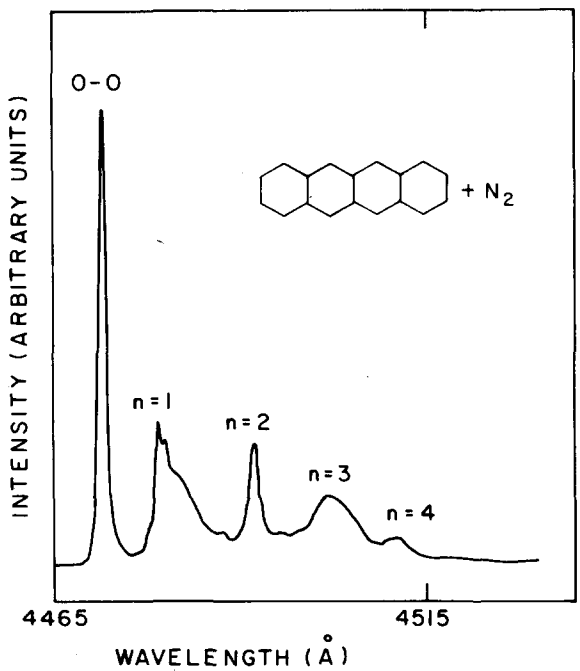

FIG. 13. An assignment of the spectral features of $T(N_2)_n$ molecules on the basis of their order of appearance.

We have conducted a preliminary study of the vdW molecules formed between tetracene and some polyatomic molecules. For this purpose Ar was employed as a diluent and was seeded both with tetracene (10^{-1} Torr) and with another polyatomic molecule M at a pressure of 20–30 Torr. New spectral features, which are neither due to the bare molecule nor to $T(Ar)_n$ complexes, were tentatively assigned to TM vdW molecules. Figure 14 shows the fluorescence excitation spectra of a tertiary mixture of tetracene and benzene expanded in Ar. The spectral feature peaking at $\delta\nu = -177$ cm^{-1} towards lower energies relative to the electronic origin of T is tentatively assigned to $T(C_6H_6)$. The fluorescence excitation spectrum of tetracene and water expanded in Ar (Fig. 15) reveals, apart from TAr_1 and TAr_2 complexes, new spectral features at $\delta\nu = 100$ cm^{-1}, which are attributed to TH_2O. The limited information on the TC_6H_6 and TH_2O molecules is of interest, as it demonstrates the potential of the spectroscopic techniques employed herein for the study of solvation effects which are of real chemical interest. The currently available meager information will be supplemented by detailed studies of the formation kinetics and energetics of these interesting complexes.

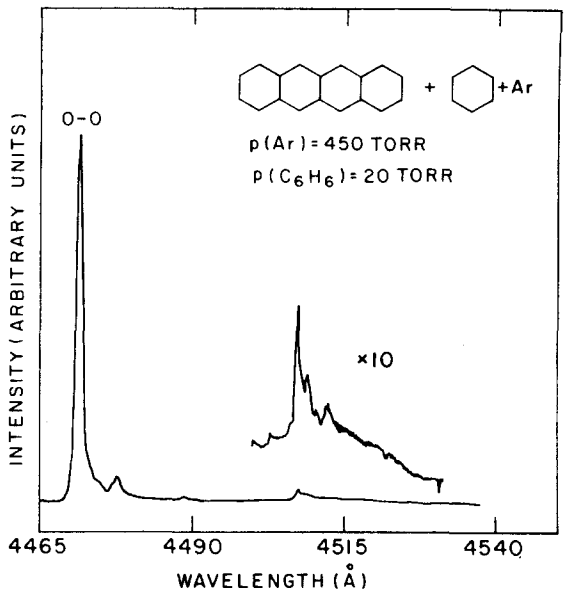

FIG. 14. Fluorescence excitation spectrum of tetracene (p = 0.1 Torr) and benzene (p = 20 Torr) expanded in 450 Torr of Ar through a 150 μ nozzle. The spectral features around 4507 Å are tentatively assigned to the T(C_6H_6) complex.

VII. LOW-ENERGY VIBRATIONAL EXCITATIONS OF TR_n MOLECULES

Up to this point we have been concerned with the vibrationless 0–0 excitations of TR_n and other vdW molecules containing tetracene. With increasing of the excitation energy, vibrationally excited states of these vdW molecules will be exhibited in the fluorescence excitation spectrum. In what follows we shall present some spectroscopic information on vibrational excitations of the TR_n molecule. The lowest vibrational excitations of the bare tetracene molecule are located at the energies of 245, 265, 288, and 314 cm^{-1} above the electronic origin,[26] the first three vibrational excitations being very weak, while the 314 cm^{-1} vibrational excitation is strong, with an intensity of 0.40 relative to that of the electronic origin. Figures 16 and 17

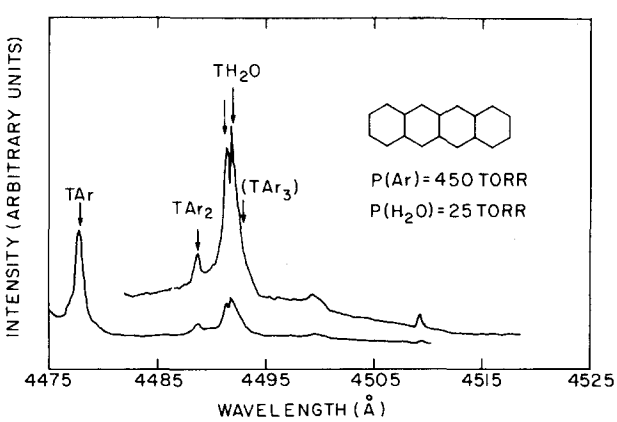

FIG. 15. Fluorescence excitation spectrum of tetracene (p = 0.1 Torr) and water (p = 25 Torr) expanded in 450 Torr of Ar through a 150 μ nozzle. The spectral features of the TAr_n complexes are marked by arrows. The new spectral features at 4491 Å are tentatively assigned to the T(H_2O) complex.

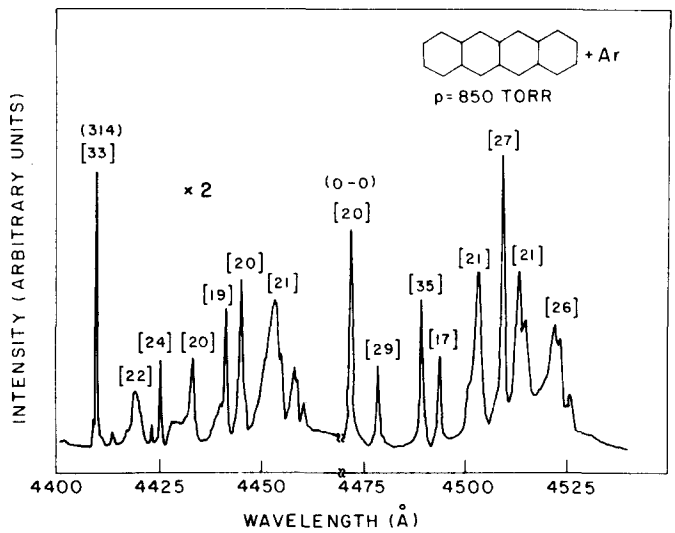

FIG. 16. Fluorescence excitation spectrum in the region 4400–4525 Å of tetracene (0.1 Torr) expanded in 850 Torr of Ar. The vibrationless electronic excitation to S_1 of the bare T molecule is marked by (0–0), while the 314 cm^{-1} vibrational excitation in the S_1 manifold of bare T is marked by (314). The spectral features appearing on the low energy side of the 0–0 band are due to the vibrationless excitations of TAr_n complexes, while the bands in the range 4419–4460 Å (see Table IV) are attributed to ~ 314 cm^{-1} vibrational excitations of the TAr_n molecules. The numbers in square brackets [ ] present the decay lifetimes (in nsec) of the photoselected states.

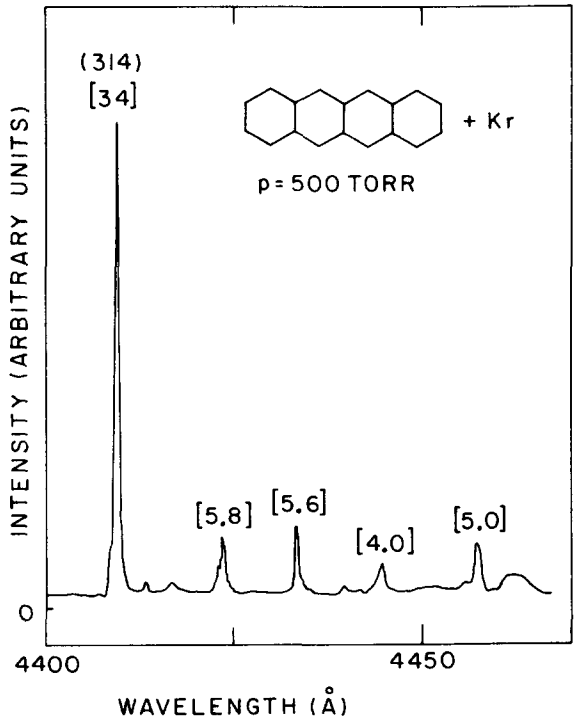

FIG. 17. Fluorescence excitation spectra in the region 4405–4460 Å of tetracene (0.1 Torr) expanded in 500 Torr of Kr. The 314 cm^{-1} vibrational excitation in the S_1 electronic state of the bare T molecule is marked by (314). The four pronounced spectral features appearing on the low energy side of the (314) band are attributed to ~ 314 cm^{-1} vibrational excitations of TKr_n molecules (see Table IV). The numbers in square brackets [ ] present the decay times (in nsec) of the photoselected states.

TABLE IV. Excited-state energetics of the 314 cm^{-1} vibrational excitation of TR_n molecules.

Molecules	n[a]	λ (Å)	$\delta\bar{\nu}$[b] (cm^{-1})
	0	4409.7	0
	(1)	4419.0	47
	(2)	4425.1	79
TAr_n	(3)	4433.0	119
	(4)	4441.2	161
		4445.0	180
		4453.0	221
		4458.0	246
		4460.4	258
	0	4409.7	0
TKr_n	(1)	4424.0	74
	(2)	4433.5	122
	0	4409.7	0
TXe_n	(1)	4428.2	95
	(2)	4446.2	186

[a]Assigned according to order of appearance of bands.

[b]Red shift of vibrational excitation of TKr_n from the 314 cm^{-1} vibrational excitation of bare T. Accuracy is ± 3 cm^{-1}.

show the fluorescence excitation spectra of $T(Ar)_n$ and $T(Kr)_n$ molecules at the low energy side of the 314 cm^{-1} vibration of the bare tetracene molecule. These spectral features are attributed to the vibrational excitations of the TR_n molecules, this vibrational excitation being close to 314 cm^{-1}. On the basis of the order of appearance of these spectral features, we were able to assign them to individual TR_n (R = Ar, Kr, and Xe) molecules. The results of this analysis are presented in Table IV. The spectral shifts $\delta\bar{\nu}$ of these vibrational excitations of TR_n molecules relative to the 314 cm^{-1} vibrational excitation of the bare T molecule are similar to but not identical with the spectral shifts $\delta\nu$ exhibited by the vibrationless excitations of the same molecules with respect to the electronic origin of T. The energy difference $(\delta\bar{\nu} - \delta\nu)$ represents the shift of the frequency of the 314 ± 2 cm^{-1} vibration of the tetracene molecule upon complexing. The values of $(\delta\bar{\nu} - \delta\nu)$ are rather small, e.g., in the range -10 to $+10$ cm^{-1} (with an accuracy of ± 5 cm^{-1}) and do not reveal any systematic trends. Further work on microscopic solvent effects on the vibrational frequencies of a large molecule in a vdW complex will be of interest. However, for the time being, we shall utilize this spectroscopic information to provide the input data for studies of intramolecular vibrational energy flow in the S_1 state of TR_n molecules, which will be reported in Sec. IX.

VIII. ELECTRONIC RELAXATION IN TR_n MOLECULES

The decay lifetimes of TR_n molecules are expected to provide information on solvent perturbations on intramolecular electronic radiationless transitions in electronically excited states of large molecules. These studies of electronic relaxation in well-characterized TR_n molecules in their S_1 state are of interest in the elucidation of the mechanisms of intersystem crossing (ISC) in the statistical limit and, in particular, for the understanding of the external heavy atom effect on ISC in large molecules. A preliminary report on the observation of the external heavy atom effect in vdW molecules has already been reported[16] and in what follows our detailed experimental results concerning time-resolved and quantum yield data will be presented. We have studied the time-resolved fluorescence following photoselective excitation (pulse spectral bandwidth of 0.3 cm^{-1} and temporal Gaussian profile with FWHM of 4 nsec)[26] of the electronic origin and the 314 cm^{-1} vibrational excitations of the bare T molecule, of the electronic origins of the TR_n complexes, as well as the vibrational excitations of TR_n molecules. The time-resolved decay curves for the TR_n (R = Ne, Ar, and Kr) molecules exhibited a single exponential decay over a time scale up to 100 nsec. The decay lifetimes of the low-lying excitations of the bare molecule, and for the TR_n (R = Ne, Ar, and Kr) molecules are presented in Figs. 4 and 16–18 and are summarized in Table V.

A. Decay lifetimes of the TNe_1 and TAr_n molecules

One of the predictions of the theory[8] of intramolecular electronic relaxation (ER) in large molecules is that for a large molecule corresponding to the statistical limit the ER rate is not modified by solvent perturbations, provided that three conditions are satisfied.

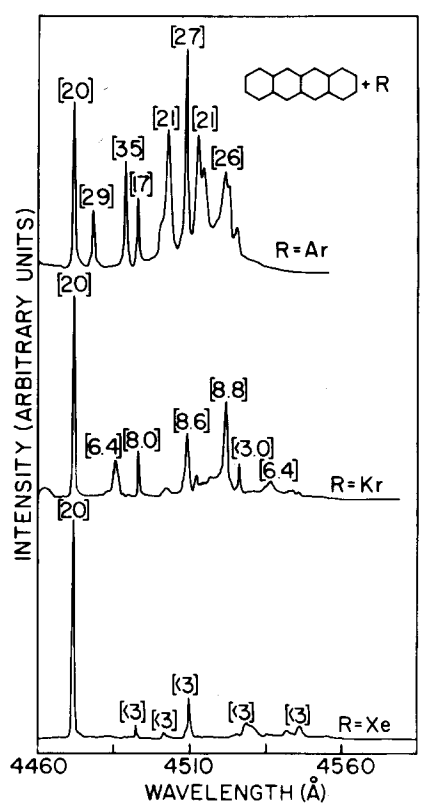

FIG. 18. Fluorescence excitation spectra of vibrationless excitations of TR_n molecules (R = Ar, Kr, and Xe). The numbers in square brackets [ ] present the decay lifetimes (in nsec) of the excited states of the individual TR_n molecules.

TABLE V. Decay lifetimes for the vibrationless excited state of TR_n molecules.

Molecule	τ[a] (nsec)	$\ll\tau\gg$[b] (nsec)
T	19	...
TNe_1	33	...
TAr_1	29	
TAr_2	35	
TAr_3	17	
TAr_4	21	...
TAr_5	27	
TAr_6	21	
TAr_7	26	
TKr_1	6.4	
TKr_2	8.0	9±1
TKr_3	8.6	
TKr_4	8.8	
TXe_1	<3	1.5±0.4
TXe_2	<3	

[a]Direct determination from time-resolved data. Accuracy is ±10%.
[b]Inferred from quantum yield data of Table VI.

First, the comparison between the ER characteristics of the isolated and the medium-perturbed molecule is conducted for the decay of the electronic origin of the excited state. Under these circumstances, one does not encounter any complications resulting from medium-induced vibrational relaxation (and vibrational excitation) of the medium-perturbed large molecule to other vibrational states, which may have different ER lifetimes.[8] Second, the molecule–solvent interaction does not modify the nuclear motion and the vibrational level structure in any of the relevant electronic configurations. Third, the solvent is "inert," which does not modify the energy levels and the intramolecular nonadiabatic and spin–orbit coupling.[8] These predictions have not yet been subjected to a critical experimental test. The absence of appreciable medium perturbations on the ER of the S_1 state of benzene,[45] naphthalene,[46,47] and anthracene[8] is considered as supporting evidence. However, all of this experimental information pertains to room temperature data, being plagued with the effects of vibrational sequence congestion, which prohibit genuine photoselective excitation of the electronic origin. To explore the effects of medium perturbations on the ER from a vibrationless excited electronic configuration of a large molecule, we have compared the lifetime of the electronic origin of the bare ultracold T molecule with the decay lifetimes of the electronic origin of vdW molecules of T with light rare gases. Complexing of a large aromatic molecule with Ne and Ar seems to satisfy the condition of medium perturbations exerted by an "inert" solvent as the spectral shifts are extremely small relative to the S_1–S_0 electronic energy gap and the light Ne and Ar atoms do not appreciably modify the spin–orbit coupling between the singlet S_1 and the triplet T_1 states, which is responsible for ISC in the "isolated" molecule, and do not change the S_1–S_0 nonadiabatic coupling, which may be responsible for internal conversion.

The lifetime of the electronic origin of the bare tetracene molecule is $\tau_0 = 19 \pm 1$ nsec, in accord with our previous data.[16,26,48] The lifetimes τ of the electronic origins of the TNe_1 and $T(Ar)_n$ complexes are close to or longer than τ_0. The variation of the lifetimes of these vdW complexes of T with light R atoms (Table V) is in the region 17 ± 2 to 35 ± 3 nsec, the value of τ varying over a numerical factor of 2. No systematic trend in the variation of these values of τ could be detected. These experimental τ values are determined by the familiar relation $(\tau)^{-1} = (\tau_r)^{-1} + (\tau_{nr})^{-1}$, where τ_r is the pure radiative lifetime, while τ_{nr} is the nonradiative lifetime due to electronic relaxation. The moderately small changes of τ of tetracene with binding of Ne and Ar can originate either from changes in τ_r or from modifications of τ_{nr}. We believe that the changes of the pure radiative lifetime upon binding of rare-gas atoms to T are minor and that the changes of the lifetimes reflect variations in the nonradiative lifetimes. The general trend of the lifetimes of the electronic origin of TNe and TAr_n is lengthening relative to τ_0, reflecting some retardation of the nonradiative decay of $S_1(0)$ upon binding of light rare-gas atoms. This effect, though relatively small, is of interest as it reflects the possible role of weak binding of rare-gas atoms to an aromatic molecule in the modification of the nuclear motion and vibrational excitations of non-totally symmetric vibrations, which are not exhibited in the absorption spectrum, but which may act as accepting modes in the ER process. These experimental data are not informative in identifying the nature of the nonradiative decay channel of the electronic origin of the S_1 state of tetracene which, on the basis of optical selection studies in the bare molecule, appears to be dominated by $S_1 \rightarrow T_1$ ISC, with a possible intermediation of the second triplet T_2 state.[26] From our results we conclude that the theoretical predictions regarding the invariance of the ER characteristics of an excited electronic origin of a large molecule to medium perturbations provides a sensible qualitative description, which has to be supplemented by more detailed theoretical studies of the effects of an inert medium on the nuclear states and the interstate coupling.

B. External heavy atom effect on intersystem crossing in TKr_n and TXe_n molecules

Figure 19 provides an overview of the decay lifetimes of the vibrationless S_1 level of a variety of TR_n molecules. From these results it is apparent that the lifetimes of the vdW molecules TKr_n and TXe_n reveal a dramatic shortening relative to τ_0, as well as relative to the lifetimes of TNe and TAr_n molecules. The decay lifetimes of individual TKr_n molecules could be directly determined by our techniques of time-resolved spectroscopy. On the other hand, the lifetimes of TXe_n complexes are too short (<3 nsec) to be determined directly. To obtain an estimate of the decay lifetimes of the TXe_n complexes we have utilized quantum yield data. The fluorescence excitation spectra of tetracene in Kr

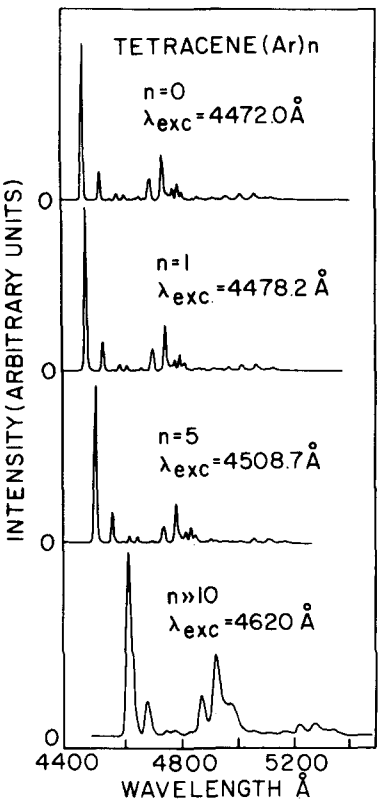

FIG. 19. Energy-resolved emission spectra from the electronic origin of the S_1 state of the bare T molecule ($n=0$), of TAr_1 ($n=1$), of TAr_5 ($n=5$), and of a large complex TAr ($n \gg 10$). The coordination numbers and the excitation energies are marked on the spectra.

(Fig. 2) and Xe (Fig. 3) were obtained by keeping the pressure of the T molecule constant and changing the stagnation pressure, while the absolute fluorescence intensity was monitored. The decrease of the relative intensities of the spectral features due to the TKr_n and TXe_n vdW molecules relative to the 0–0 bond of the bare molecule, as compared with the TAr_n system, originates from the reduction in the emission quantum yield of the vdW molecules containing heavy atoms. We can immediately utilize Eq. (IV.6) to obtain an estimate of the mean decay lifetime. We assume again that the decay lifetime of a given class of TR_n molecules is independent of the coordination number n. This assumption is consistent with the time-resolved data for the TKr_n molecules. The average value $\langle\langle\tau\rangle\rangle$ of the lifetimes of TR_n molecules is obtained from Eq. (IV.6):

$$\langle\langle\tau\rangle\rangle = \tau_0 \frac{q(p)}{r(p)-1} \quad . \tag{VIII.1}$$

The parameters $q(p)$ [Eq. (IV.7a)] and $r(p)$ [Eq. (IV.7b)] were calculated by the procedures described in Sec. IV. The values of $\langle\langle\tau\rangle\rangle$ calculated from the quantum yield data (Table VI) for TKr_n reveal two features. First, the mean lifetimes for the TKr_n molecules $\langle\langle\tau\rangle\rangle = 9$ nsec estimated from the quantum yields are in reasonable agreement with the lifetimes in the range 6.0–9.0 nsec obtained from direct time-resolved data for these molecules. Second, the mean lifetime for the TKr_n molecules estimated from the quantum yield data is practically independent of the stagnation pressure p. Since at higher values of p the populations of the TKr_n molecules shift towards higher values of n, we can conclude that the invariance of $\langle\langle\tau\rangle\rangle$ with increasing p indicates that the lifetimes are only weakly dependent on the coordination number n, which is in accord with the time-resolved data for the TKr_n molecules. For the TXe_n molecules the only quantitative information emerges from the quantum yield data. The mean decay lifetime for TXe_n molecules is $\langle\langle\tau\rangle\rangle \simeq 1.5$ nsec. The mean decay lifetime is again invariant with respect to changes in the stagnation pressure, so we can conclude that for the TXe_n molecules the decay lifetimes are practically independent of the coordination number.

The dramatic shortening of the decay lifetimes of the TKr_n and TXe_n molecules brings these decay lifetimes into the range $\tau \ll \tau_r$, where $\tau_r \simeq 35$ nsec is the (estimated) pure radiative lifetime.[26] Accordingly, the ex-

TABLE VI. Mean decay lifetimes $\ll\tau\gg$ for TKr_n and TXe_n estimated from emission quantum yields.

Diluent	P (Torr)	$A_0(\bar{p})/A_0(p)$	$r(p)$	$q(p)$	$\ll\tau\gg/\tau_0$	$\ll\tau\gg$ (nsec)
Kr	$\bar{p}=135$	1.00	1.24	...	...	...
Kr	275	2.00	2.48	0.71	0.48	9.1
Kr	330	3.00	3.72	1.33	0.49	9.3
Kr	391	5.00	6.2	2.57	0.49	9.4
Kr	465	10.00	12.4	4.65	0.41	7.7
Xe	$\bar{P}=100$	1.00	1.56	...	...	...
Xe	153	2.00	3.12	0.133	0.063	1.2
Xe	181	3.00	4.62	0.266	0.072	1.4
Xe	218	5.00	7.80	0.632	0.093	1.8
Xe	256	10.00	15.6	1.305	0.089	1.7

perimental decay rates for TKr_n and TXe_n are dominated by the nonradiative component. The enhancement of the ER in the electronic origin of the S_1 state in TKr_n and TXe_n molecules is attributed[16] to the external heavy atom effect on the $S_1 \rightarrow T_1$ ISC in the T molecule, which is induced by the heavy rare-gas atoms. On the basis of the identification of the chemical composition of the individual TR_n molecules we were able to explore in considerable detail this solvent effect on ER. While the heavy external heavy atom effect on $T_1 \rightarrow S_0$ ISC is well documented for guest aromatic molecules in solutions of halogenated hydrocarbons[27,28] and in rare-gas solids,[32,36] the present results elucidate some microscopic features of this interesting phenomenon. Several characteristics of the lifetimes are of interest. First, the heavy atom enhancement of the ISC is considerably more effective with increasing of the nuclear charge of the perturbing heavy atom, which is expected.[27-37] Second, the shortening of the lifetimes of TKr_n and TXe_n molecules is already exhibited for $n=1$. Third, the lifetimes of the TKr_1, TKr_2, TKr_3, and TKr_4 molecules, as directly determined, are very close, showing only a very weak unsystematic charge with n. Fourth, the lifetimes of TXe_n molecules, as estimated from quantum yield data, are practically independent on the coordination number. The only exception, which we do not understand, for the general rule of the weak n dependence of the heavy atom enhanced lifetime of TKr_n and TXe_n complexes is the short decay lifetime $\tau < 3$ nsec of the TKr_n complex with $n > 4$, peaking at 4526.3 Å. In spite of this exception we can conclude that the lifetime of TKr_n and TXe_n molecules practically saturates at $n=1$ and the lifetime varies only weakly with a further increase of the coordination number beyond $n=1$.

The major conclusion emerging from these results is that the heavy atom effect, which induces the $S_1 \rightarrow T_1$ intramolecular ISC of tetracene within TKr_n ($n=1-4$) and TXe_n complexes, essentially originates from T–Kr or T–Xe pair interactions. The predominant role of T–R single-pair interactions in ISC for the singlet state of T reflects the effect of specific intermolecular interactions, which determine the consequences of solvent perturbations modifying the intrastate intramolecular coupling, on this class of ER processes. Two scrambling mechanisms were advanced[28-37] to account for the external heavy atom effect on ISC. These involve (A) mixing with neutral excitations of the heavy rare-gas atoms and (B) mixing with charge transfer states. Invoking analogies to electronic excitations in solids, mechanism (A) can be considered as mixing with Frenkel-type excitons,[49] while mechanism (B) corresponds to mixing with Wannier-type excitations.[49] Mechanism (A) for TR_n is expected to result in a cumulative contribution from n rare-gas atoms, while mechanism (B) may involve specific pair interactions. Our experimental data provide evidence for the mixing of charge transfer states as the dominating mechanism for the heavy atom enhanced $S_1 \rightarrow T$ ISC in TKr_n and TXe_n molecules. It should be pointed out, however, that this conclusion is not universal and that in vdW complexes of heavy rare-gas atoms with other aromatic molecules both scrambling mechanisms may be operative.

IX. SOME OBSERVATIONS ON INTRAMOLECULAR VIBRATIONAL ENERGY FLOW IN LARGE van der WAALS MOLECULES

The understanding of intramolecular dynamics is of considerable current interest. These studies are expected to elucidate the nature of basic reactive vibrational predissociation (VP) processes[13-15,23,24] and are relevant for establishing the general features of intramolecular vibrational energy flow in large molecules. Two general classes of intrastate dynamics of vdW molecules, which involve a single electronic confrontation, can be envisioned.

Reactive VP *processes*: When the excess vibrational energy of the vdW molecule exceeds the energy of the vdW bond, VP on a single nuclear potential surface can occur. In simple triatomic complexes,[13-15] e.g., I_2R (R = He, Ne, and Ar), the VP process involves $V \rightarrow T$ exchange. In vdW dimers containing a pair of diatomic molecules,[23(c)] VP can occur both by $V \rightarrow T$ as well as by intermolecular $V \rightarrow V+T$. Finally, in complicated vdW complexes containing a pair of polyatomic molecules, e.g., $(N_2O)_2$ dimer,[50,51] the reactive VP process may involve simultaneous $V \rightarrow T$ exchange, together with intermolecular and intramolecular $V \rightarrow V+T$ transfer[23(d)] between the two subunits. The conceptual framework for the understanding of such reactive processes is well developed, although some extensions for the study of large systems, e.g., tetrazine–Ar[11] and our TR_n systems, will be necessary. It will be interesting to obtain information regarding analogous VP reactive processes of large vdW complexes containing large aromatic molecules.

Nonreactive vibrational energy flow: When the VP decay process is slow on the relevant time scale or when the VP channel is closed because of energetic reasons, one can consider the possibility of nonreactive $V \rightarrow V$ exchange between the two subunits or within one subunit of polyatomic vdW complexes. An interesting example involves nonreactive resonant vibrational energy flow between the two subunits of a vdW dimer consisting of two halogen molecules.[23(c),52] Several other nonreactive near-resonant processes can be of considerable interest. For example, one can consider the problem of nonreactive vibrational energy flow within one large subunit of a vdW complex with the excess vibrational energy being shared by low-frequency modes of the vdW bond. This interesting and intriguing process has not yet been explored, either experimentally or theoretically. In fact, it is still an open question as to whether such a process will be amenable for experimental observation. The search for nonreactive vibrational energy flow within a subunit of the vdW complex between a large molecule and a rare-gas atom should be conducted when the excess vibrational energy is lower than the energy of the vdW bond. In such a low energy range the density of vibrational states of the composite system, i.e., intramolecular vibrations, as well as vibrational modes of the vdW bond may not be sufficiently high to ensure irreversible intramolecular vibrational energy redistribution.

We have conducted a study of intrastate dynamics of

T–Ar_n and T–Kr_n molecules excited to their S_1 state at excess vibrational energy of ~314 cm^{-1} above their electronic origin. These data demonstrate that the VP process

$$TR_n^{(v)} \rightarrow TR_{n-1}^{(v')} + R \qquad \text{(IX.1)}$$

is not exhibited at these low excess vibrational energies on the (nsec) time scale of the radiative decay. Some indirect information on nonreactive intramolecular vibrational energy flow was inferred from these results. Subsequently, we have searched for the onset of reactive VP of TKr complexes, providing some information on this process.

A. Energy-resolved emission from TAr_n molecules

Important information on the VP process (IX.1) can be obtained from energy-resolved fluorescence resulting from photoselective excitation of a well-defined vibrationally–electronically excited state of the vdW molecule. The following three classes of the energy-resolved fluorescence spectra are expected:

(1) Photoselection of the electronic origin of a vdW molecule will result in resonance fluorescence from this molecule.

(2) Photoselection of a vibrationally excited state of a vdW complex, where VP is slow or the VP channel is closed, will again lead to resonance fluorescence from the vibrationally excited molecule.

(3) Photoselection of a vibrationally excited state v of the vdW complex, where VP [Eq. (IX.1)] is efficient, will result in fluorescence from a lower-lying v' state of the vdW molecule.

To obtain information concerning resonance fluorescence from TAr_n vdW molecules [class (1)] we have measured the energy-resolved emission resulting from excitation of the electronic origin of individual molecules. The excitation energies were chosen according to the assignment in Table III. Figure 19 presents the energy-resolved emission from the vibrationless level of the bare tetracene molecule, as well as from the vibrationless level of several TAr_n molecules. The emission spectrum of the bare molecule[26] is characteristic of small configurational changes between S_1 and S_0 states, being dominated by the 0–0 transition. The emission spectra (Fig. 19) for the TAr_n molecules bear a close resemblance to that of the bare molecule, being characterized by a very similar intensity distribution. However, the dominating 0–0 feature in the emission of TAr_n shifts to lower energies with increasing n. This result is just what one expects for resonance fluorescence from TAr_n. As is evident from Table VII, the shift ΔE_e of the 0–0 peak of the emission from the vibrationless level of TAr_n from the 0–0 peak of the emission of the bare molecule is in good agreement with the spectral shift $\delta\nu$ between the electronic origins of TAr_n and T in the fluorescence excitation spectra. From this study of class (1) energy-resolved fluorescence, two additional conclusions emerge. First, the observation of resonance fluorescence from these lower-energy electronically excited states of TAr_n provides additional (though maybe somewhat redundant) support to their assignment as vibrationless states of the complexes. Second, the close family resemblance between the energy-resolved emission spectra (Fig. 19) of T and TAr_n, as far as relative intensities are concerned, indicates that the intramolecular Franck–Condon factors are not modified by the binding of rare-gas atom(s) to a large aromatic molecule. One can thus assert that intramolecular configurational equilibrium changes between the S_1 and S_0 states for the optically active modes of this large molecule are practically unchanged by vdW bonding, as is expected.

TABLE VII. Spectral shift of the energy of the $\Delta v = 0$ emission of TAr_n molecules from the 0–0 emission of bare T.

Vibrational excitation in S_1	Coordination number n[a]	λ_{exc}[b] (Å)	ΔE_e[c] (cm^{-1})	$\delta\nu$[d] (cm^{-1})
Electronic origin	0	4471.6	0±10	0
	1	4478.2	50±15	35±2
	2	4488.0	72±15	88±2
	5	4508.0	215±25	184±2
314 cm^{-1}	0	4409.9	0±10	0
	1	4419.8	40±15	35±2
	2	4425.0	70±15	88±2
	3	4433.3	98±15	108±2
	4	4441.1	122±20	155±2
		4445.0	146±20	184±2
		4453.8	172±20	

[a]Coordination numbers from analysis of Sec. III (Table III).
[b]Excitation wavelength for energy-resolved emission.
[c]Shift towards lower energies of the peak of the $\Delta v = 0$ band of TR_n from the peak of 0–0 emission of T.
[d]Red spectral shift of vibrationless TAr_n band (from Table III).

More interesting are the energy-resolved emission spectra resulting from photoselective excitation of TAr_n molecules at an excess vibrational energy of ~314 cm^{-1}. The fluorescence excitation spectra of these molecules were reported in Sec. VII, while Figs. 20 and 21 display the energy-resolved emission spectra, together with those for the bare molecule. Excitation of the bare molecule to the S_1 state at an excess vibrational energy of 314 cm^{-1} results in a fluorescence peak of moderate intensity towards lower energies by the intense $\Delta v = 0$ emission. The shift of the $\Delta v = 0$ emission from the S_1 (314 cm^{-1}) relative to the 0–0 emission peak for the $S_1(0)$ is 10 cm^{-1}. This negligibly small shift is compatible with the very small change in the vibrational frequency of the 314 cm^{-1} between the S_1 and S_0 states.[26] Photoselective excitation of TAr_1 at excess vibrational energy, which corresponds to the 314 cm^{-1} vibration, results in an interesting energy-resolved emission (Fig. 20), which exhibits the following features:

(a) A weak emission band corresponding to resonance fluorescence is exhibited followed by an intense $\Delta v = 0$ emission band.

(b) The relative intensity of the resonance fluorescence band of TAr_1 relative to the intensity of $\Delta v = 0$ is lower than the corresponding relative emission in-

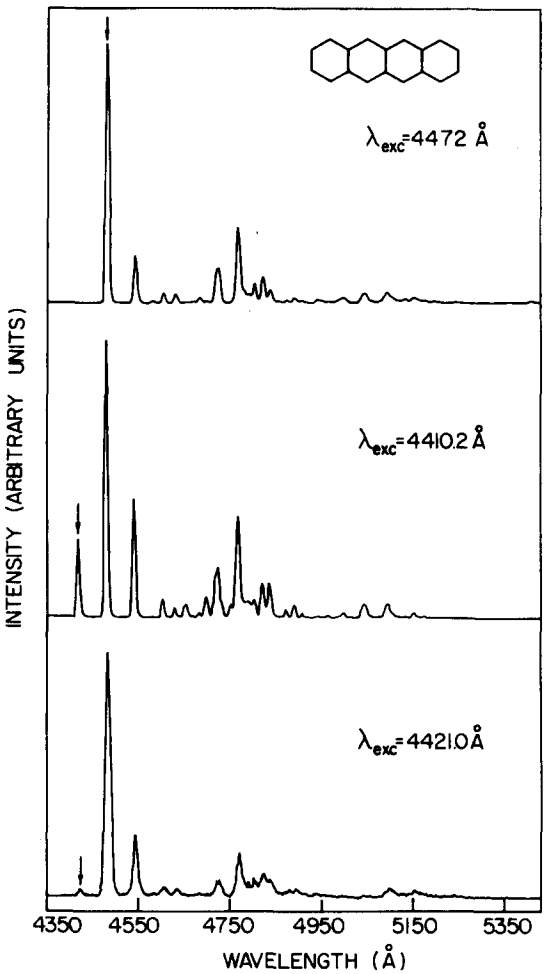

FIG. 20. Energy-resolved emission spectra from the electronic origin and the 314 cm^{-1} vibrational excitation of bare T and from the ~314 cm^{-1} vibrationally excited state of TAr_1. The position of the laser excitation is marked by an arrow. The resonance fluorescence is genuine as determined by energy- and time-resolved studies.

tensities in the bare molecule.

(c) The $\Delta v = 0$ emission peak of TAr_1 is shifted by $\Delta E_e = 40 \pm 15$ cm^{-1} towards lower energies from the 0–0 emission peak of the bare molecule.

(d) The $\Delta v = 0$ emission peak of TAr_1 seems to be broadened relative to the 0–0 emission from the vibrationless state of TAr_1.

Observation (c) implies that the VP process

$$TAr_1(v = 314\ cm^{-1}) \rightarrow T(v = 0) + Ar \qquad (IX.2)$$

did not take place on the time scale of the decay $\tau = 22 \pm 2$ nsec (see Fig. 16) of this 314 cm^{-1} excitation of TAr_1, since the occurrence of VP would have resulted in $\Delta E_e = 0$. However, on the basis of the invariance of the intramolecular Franck–Condon factors with respect to vdW binding of Ar atoms, we would have expected that the spectral distribution of the resonance fluorescence from the TAr_1 ($v = 314$ cm^{-1}) will be characterized by an intensity distribution which is practically identical with that for emission from the T ($v = 314$ cm^{-1}) bare molecule. This expectation is in contrast with observation (b). A way out of this difficulty is to propose that nonreactive intramolecular vibrational energy flow has occurred in the TAr_1 ($v = 314$ cm^{-1}) molecule, the intramolecular 314 cm^{-1} vibrational excitation has been degraded to one of the lower lying 288, 265, or 245 cm^{-1} intramolecular vibrations, which were identified,[26] or to another low-frequency vibration, while the excess vibrational energy has been transferred to a bond vibrational motion of the T–Ar vdW bond. Such a mechanism will require near-resonant interaction between the intramolecular energy differences and the frequencies of the vdW bond. A similar conclusion concerning the inefficiency of the VP of the TAr_2 complex on the time scale of its decay ($\tau = 24 \pm 2$ nsec, see Fig. 16)

$$TAr_2(v = 314\ cm^{-1}) \rightarrow TAr_1(v = 0) + Ar \qquad (IX.3)$$

is obtained from the examination of the experimental value of ΔE_e (Table VII). The VP of TAr_2 ($v = 314$ cm^{-1}), according to Eq. (IX.3) and resulting in TAr_1 ($v = 0$), is expected to result in ΔE_e, which is equal to $\delta\nu(n = 1)$. The experimental result (Table VII) is $\Delta E_e = \delta\nu(n = 2)$, indicating that process (IX.3) does not occur.

We thus conclude that vibrational excitation of TAr_1 and TAr_2 at the excess vibrational energy of 314 cm^{-1}

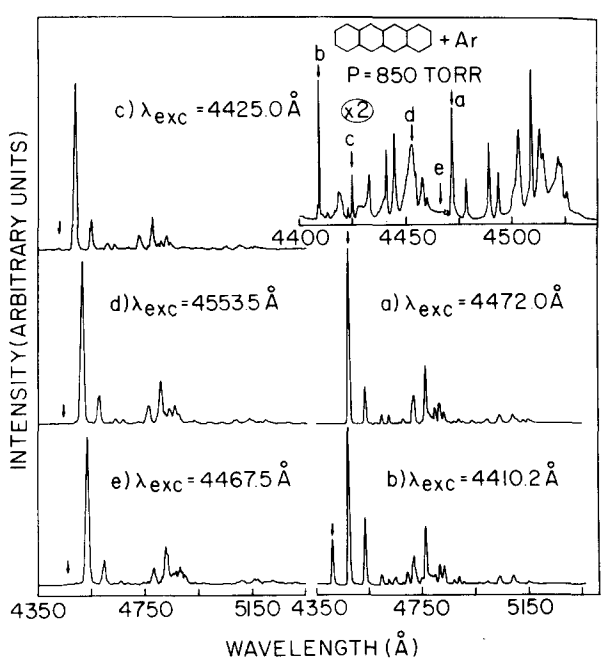

FIG. 21. Energy-resolved emission from several ~314 cm^{-1} vibrationally excited states of some TAr_n molecules. The upper insert provides the fluorescence excitation spectrum of T and TAr_n, where the five excitation wavelengths are marked by arrows. Spectrum (a), which corresponds to the energy-resolved emission from the electronic origin of T, and spectrum (b), which corresponds to energy-resolved emission from the 314 cm^{-1} vibrational excitation of T, are displayed for the sake of comparison. Spectrum (c) corresponds to energy-resolved emission from the 314 cm^{-1} vibrational excitation of TAr_2, while spectra (d) and (e) give the energy-resolved emission from the 314 cm^{-1} vibrational excitation of TAr_n complexes with high coordination numbers. The position of the laser excitations are marked by arrows.

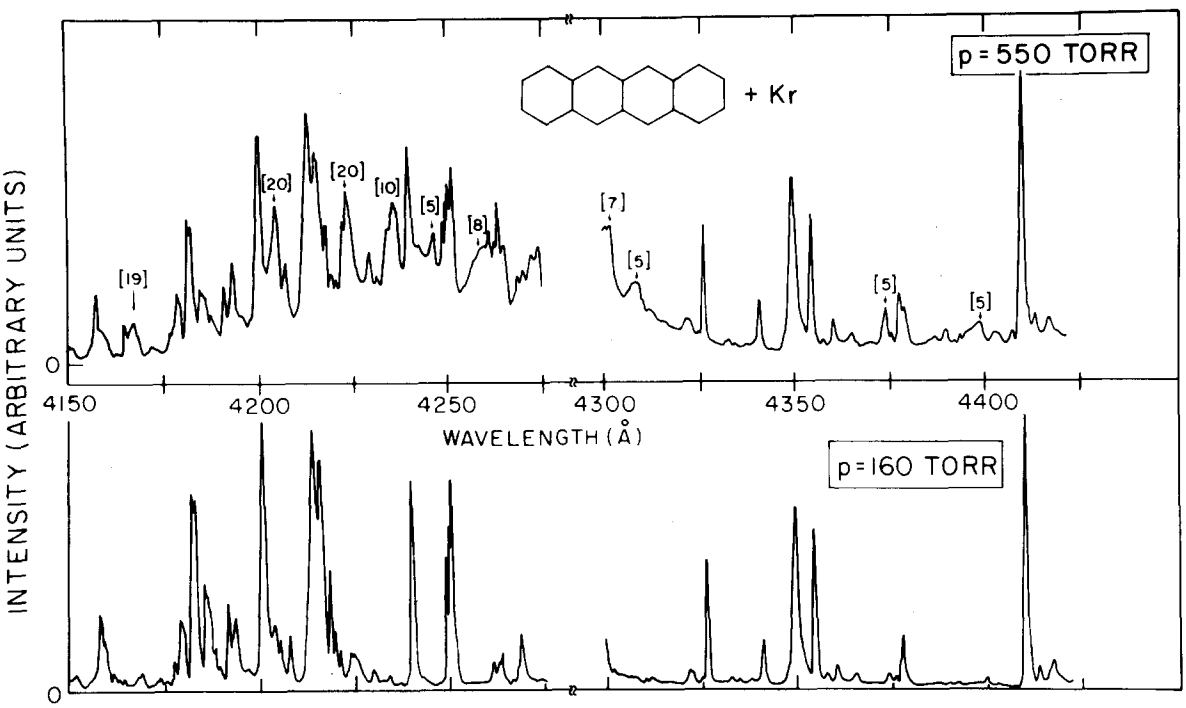

FIG. 22. Fluorescence excitation spectra of tetracene in the range 4150–4460 Å, expanded in Kr at $p = 160$ and 550 Torr. The spectrum at $p = 550$ Torr reveals electronic–vibrational excitation of Kr_n molecules, whose lifetimes were measured. The numbers in square brackets [ ] represent the decay lifetimes (in nsec). Note the dramatic lengthening of the decay lifetime at wavelengths below 4260 Å.

does not result in VP of an Ar atom. The inefficiency of VP may be blamed on one of the following effects: (i) energetic: the binding energy of the Ar atom in the TAr_n molecules exceeds the vibrational energy of 314 cm^{-1}; (ii) dynamic: the VP channel is open, but the VP rate is slow on the (nsec) time scale. We prefer possibility (i), as the model calculations by Ondrechen *et al.*[43] for the binding of TAr_n complexes indicate that the binding of Ar to tetracene is 550 cm^{-1}, so that the VP channels (IX.2) and (IX.3) are closed.

B. Vibrational predissociation of TKr

We have studied the VP of tetracene–krypton complexes by taking advantage of the heavy atom effect (Sec. VIII.B) which considerably shortens the experimental radiative lifetimes of TKr_n molecules. The decay lifetimes of the electronic origin and of the 314 cm^{-1} excitation in the S_1 state of the bare T molecule are 19 ± 2 and 33 ± 3 nsec, respectively, and vary quite slowly with excess vibrational energy up to 1000 cm^{-1}, while the decay lifetimes of the electronic origin and the 314 cm^{-1} excitation of TKr_n complexes (see Figs. 17 and 18) were found to be in the range 6.0–8.0 nsec. Accordingly, a time-resolved measurement of the decay lifetime, following excitation of a vibrational excitation of a TKr_n complex, will immediately reveal whether VP has occurred on the time scale of the radiative decay. A lifetime in the range 5.0–8.0 nsec originates from a dressed TKr_n complex, while a lifetime in the range 20–30 nsec originates from a liberated T molecule, produced by VP of the TKr complex. Figure 17 reveals the lifetimes of the 314 cm^{-1} vibrationally excited state of the TKr_n complexes which are all in the range 6.0–8.0 nsec, as is appropriate for emission from the dressed molecules. In particular, it is important to note that the time-resolved emission from the TKr_1 band at 4424.0 Å results in a short 6.0 nsec lifetime, so that the VP of this molecule with excess vibrational energy of 314 cm^{-1} does not occur. This result is expected, as the absence of VP from the 314 cm^{-1} excitation of TAr_1 (Sec. IX A) suggests that the 314 cm^{-1} excitation of TKr_1, which is characterized by a stronger vdW binding energy, is also stable with respect to reactive VP.

We have conducted a semiquantitative search for the onset of VP in vibrationally excited krypton complexes, while climbing up the vibrational ladder. Figure 22 shows the fluoresence excitation spectrum of tetracene expanded in $p = 160$ Torr Kr for excess vibrational energies 300–2000 cm^{-1} above the electronic origin, which is practically uncontaminated by TKr_n molecules, together with a spectrum of tetracene expanded in 550 Torr Kr, which shows substantial complexing. A cursory comparison of the two spectra in Fig. 22 immediately reveals the spectral features due to vdW complexes. We have conducted studies of time-resolved emission from spectral features due to tetracene–krypton complexes. Up to excess vibrational energies of 1200 cm^{-1} the decay lifetimes of the Kr complexes are in the range 5.0–8.0 nsec, originating from "dressed" complexes. Excitation at excess vibrational energies exceeding 1250 cm^{-1} results in a dramatic lengthening of the decay lifetimes, which are now 20 ± 2 nsec in the excess energy range 1250–2200 cm^{-1},

clearly demonstrating that the excitation of the (as yet unidentified) TKr_n complexes in this higher energy range results in effective VP on the time scale of ~6 nsec. From these experimental data, we can set an upper limit for the dissociation energy of the T–Kr vdW bond in the S_1 electronically excited state $D_e(T-Kr) < 1250\ cm^{-1}$. This estimate of the upper limit for the dissociation energy of the T–Kr vdW bond is consistent with some recent model calculations.[43] Ondrechen *et al.*[43] have calculated the binding energy of the TKr_1 molecule in the ground S_0 state to be $D_0(T-Kr) = 660\ cm^{-1}$. Setting $D_e(T-Kr) = D_0(T-Kr) + \delta\nu\ (n=1)$, the theoretical estimate together with the spectral shift in Table III result in the estimate $D_e(T-Kr) = 730\ cm^{-1}$, in accordance with the experimental upper limit for the excited-state dissociation energy.

ACKNOWLEDGMENT

We are grateful to Professor S. A. Rice for useful comments concerning the solubility of aromatic molecules in rare gases.

[1]H. C. Longuett Higgins and J. A. Pople, J. Chem. Phys. **27**, 192 (1957).
[2]S. Basu, in *Advances in Quantum Chemistry*, edited by P. O. Lowdin (Academic, New York, 1964), Vol. I, p. 145.
[3]W. Liptay, in *Modern Quantum Chemistry, Part II*, edited by O. Sinanoglu (Academic, New York, 1965), p. 173.
[4]B. Meyer, in *Low Temperature Spectroscopy* (Elsevier, New York, 1971).
[5]T. B. Birks, *Photophysics of Aromatic Molecules* (Wiley-Interscience, New York, 1970).
[6]A. Tramer and A. Nitzan, in *Photoselective Chemistry*, edited by J. Jortner, R. D. Levine, and S. A. Rice, Advances in Chemical Physics Series (Wiley-Interscience, New York, 1981).
[7]K. F. Freed, in *Photoselective Chemistry*, edited by J. Jortner, R. D. Levine, and S. A. Rice, Advances in Chemical Physics Series (Wiley-Interscience, New York, 1981).
[8]J. Jortner and S. Mukamel, in *MTP Series of Physical Chemistry*, edited by A. D. Buckingham and C. A. Coulson (Butterworths, London, 1976).
[9]F. Legay, *Chemical and Biochemical Applications of Lasers* (Academic, New York, 1977), Vol. 2.
[10]W. Klemperer, Ber. Bunsenges. Phys. Chem. **78**, 127 (1974).
[11]J. K. Kenny, D. V. Brunbaugh, and D. H. Levy, J. Chem. Phys. **71**, 4757 (1979).
[12]K. E. Johnson, L. Wharton, and D. H. Levy, J. Chem. Phys. **69**, 2719 (1978).
[13]D. H. Levy, in *Photoselective Chemistry*, edited by J. Jortner, R. D. Levine, and S. A. Rice, Advances in Chemical Physics Series (Wiley-Interscience, New York, 1981).
[14]D. H. Levy, L. Wharton, and R. E. Smalley, Acc. Chem. Res. **10**, 134 (1977).
[15]D. H. Levy, L. Wharton, and R. E. Smalley, *Chemical and Biochemical Applications of Lasers* (Academic, New York, 1977), Vol. 2, p. 1.
[16]A. Amirav, U. Even, and J. Jortner, Chem. Phys. Lett. **67**, 9 (1979).
[17]J. E. Kenny, K. E. Johnson, W. Shafrin, and D. H. Levy, J. Chem. Phys. **72**, 1109 (1980).
[18]J. A. Blazy, B. M. De Koren, T. D. Russell, and D. H. Levy, J. Chem. Phys. **72**, 2439 (1980).
[19]T. A. Milne and F. T. Greene, J. Chem. Phys. **47**, 4095 (1967).
[20]A. Amirav, U. Even, and J. Jortner, Chem. Phys. Lett. **72**, 16 (1980).
[21]S. L. Holmgren, M. Walden, and W. Klemperer, J. Chem. Phys. **69**, 1661 (1978).
[22]J. M. Huston, A. E. Barton, P. R. R. Langridge-Smith, and B. J. Howard, Chem. Phys. Lett. **73**, 218 (1980).
[23]J. A. Beswick and J. Jortner, (a) J. Chem. Phys. **68**, 2227 (1978); (b) **69**, 512 (1978); (c) **71**, 4737 (1979); (d) J. Chem. Phys. (in press).
[24]J. A. Beswick and J. Jortner, in *Photoselective Chemistry*, edited by J. Jortner, R. D. Levine, and S. A. Rice, Advances in Chemical Physics Series (Wiley-Interscience, New York, 1981).
[25]A. Amirav, U. Even, and J. Jortner, Chem. Phys. (in press).
[26]A. Amirav, U. Even, and J. Jortner, J. Chem. Phys. **74**, 3745 (1981).
[27]M. Kasha, J. Chem. Phys. **20**, 71 (1952).
[28]S. P. McGlynn, T. Azumi, and M. Kimoshita, *Molecular Spectroscopy of the Triplet State* (Prentice-Hall, Englewood Cliffs, 1969).
[29]H. Tsubomura and R. S. Mulliken, J. Am. Chem. Soc. **82**, 5966 (1960).
[30]S. H. Lin and D. Tweed, Int. J. Quantum Chem. **35**, 315 (1969).
[31]K. C. Lin and S. H. Lin, Mol. Phys. **21**, 1105 (1971).
[32]J. N. Murrell, Mol. Phys. **3**, 319 (1960).
[33]G. W. Robinson, J. Chem. Phys. **46**, 572 (1967).
[34]G. J. Hoijtink, Mol. Phys. **3**, 67 (1960).
[35]S. P. McGlynn, R. Sunseri, and N. D. Christodoules, J. Chem. Phys. **37**, 1818 (1962).
[36](a) G. W. Robinson, J. Mol. Spectrosc. **6**, 58 (1961); (b) G. W. Robinson and R. P. Frosch, J. Chem. Phys. **38**, 1187 (1963).
[37]Y. P. Hsu and P. M. Johnson, J. Chem. Phys. **59**, 136 (1973).
[38]H. Inokuchi and H. Akamutu, in *Solid State Physics*, edited by F. Seitz and D. Turnbull (Academic, New York, 1961), Vol. 12, p. 93.
[39]A. D. King and W. W. Robertson, J. Chem. Phys. **37**, 453 (1962).
[40]R. E. Smalley, L. Wharton, and D. H. Levy, J. Chem. Phys. **66**, 2750 (1977).
[41]R. J. Gordon, Y. T. Lee, and D. R. Herschbach, J. Chem. Phys. **54**, 2393 (1971).
[42]D. L. Bunker, J. Chem. Phys. **32**, 1001 (1962).
[43]M. J. Ondrechen, Z. Berkowitch-Yellin, and J. Jortner, J. Am. Chem. Soc. (in press).
[44]M. J. Ondrechen and J. Jortner (to be published).
[45]G. B. Kistiakowski and C. S. Parmenter, J. Chem. Phys. **42**, 2942 (1965).
[46]H. Schröder, H. J. Neusser, and E. W. Schlag, Chem. Phys. Lett. **54**, 4 (1978).
[47]B. Soep, C. Michel, A. Tramer, and L. Lindquist, Chem. Phys. **2**, 293 (1973).
[48]A. Amirav, U. Even, and J. Jortner, J. Chem. Phys. **71**, 2319 (1979).
[49]R. S. Knox, *Theory of Excitons* (Academic, New York, 1964).
[50]J. A. Beswick and J. Jortner, J. Chem. Phys. **74**, 6725 (1981).
[51]T. E. Gough, R. E. Miller, and G. Scoles, J. Chem. Phys. **69**, 1588 (1978).
[52]D. A. Dixon and D. R. Herschbach, Ber. Bunsenges. Phys. Chem. **81**, 145 (1977).